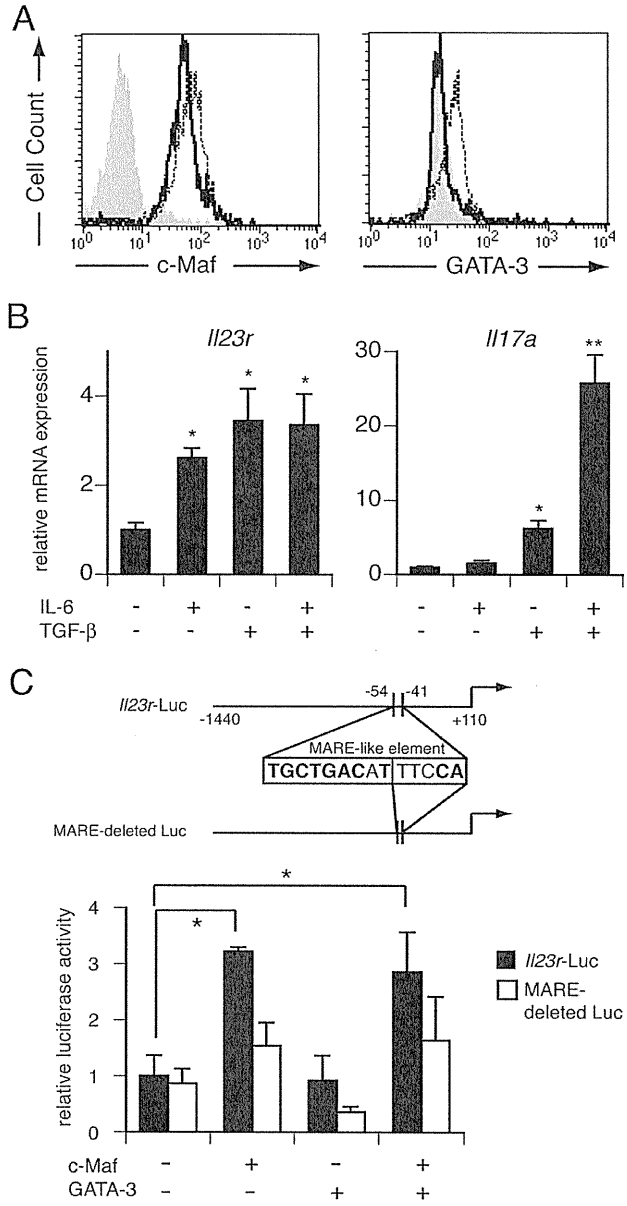

FIGURE 2. **Distinct expression patterns of c-Maf and GATA-3 in Th2 and Th17 cells and effects of these molecules on *Il23r* promoter.** *A*, flow cytometry analysis of c-Maf and GATA-3 expression in Th2 and Th17 cells. Although c-Maf expression was detected in both Th2 (*dotted line*) and Th17 (*solid line*) cells, GATA-3 expression was restricted to only Th2 cells. The *shaded areas* represent unstained Th2 cells (negative staining). *B*, qRT-PCR analysis of *Il23r* and *Il17a* expressions in naive $CD4^+$ T cells cultured for 3 days in the presence or absence of 10 ng/ml IL-6 and 3 ng/ml TGF-β. Anti-IFN-γ Ab and anti-IL-4 Ab (10 μg/ml each) were added to the culture. Either IL-6 or TGF-β is necessary for *Il23r* expression, but both cytokines are evidently necessary for significant *Il17a* induction. *C*, promoter analysis of *Il23r*. The 5′-flanking region of *Il23r* has a MARE-like sequence. (*Boldface letters* in the *box* correspond to MARE consensus sequences.) The forced expression of c-Maf had a positive effect on promoter activity, but that of GATA-3 did not. Furthermore, c-Maf did not significantly induce the luciferase activity of the deletion mutant lacking the MARE-like element, suggesting that c-Maf directly binds to this site. Data represent three independent experiments. *, $p < 0.05$.

it induced *Il17a* only slightly (Fig. 2*B*). Thus, *Il23r* is a candidate gene positively regulated by c-Maf.

Promoter Analysis of Putative c-Maf Target Genes—To obtain further insight, we performed luciferase promoter analysis using the promoters of the two genes. c-Maf overexpression induced the promoter activity of *Il23r*. c-Maf binds to a sequence called the Maf recognition element (MARE) (26). Indeed, the promoter region of *Il23r* contained a MARE-like sequence, and the deletion mutant luciferase vector that lacks the element lost responsiveness to c-Maf (Fig. 2*C*). Thus, c-Maf likely regulates Th17 proliferation via IL-23R induction. On the other hand, an ~1500-bp 5′ flanking region of *Il17a* responded to neither c-Maf nor GATA-3, suggesting that IL-17 is not a direct target of these factors (data not shown).

Ex Vivo Analysis of c-Maf Transgenic Mice—To confirm the hypothesis that c-Maf plays important role(s) in Th17 differentiation, we employed T cell-specific c-Maf Tg mice (17). As expected, the expression of IL-23R and IL-17 at the mRNA level was highly up-regulated in Tg Th cells. The expression of IFN-γ was also significantly up-regulated in Tg Th cells, but that of IL-4 was not (Fig. 3*A*). Flow cytometric analysis confirmed that the numbers of both IFN-γ-positive cells and IL-17-positive cells, but not that of IL-4-positive cells, were increased among Tg Th cells (Fig. 3*B*). To our surprise, although c-Maf Tg Th cells produced significantly more IL-17 than control cells *in vitro*, this difference disappeared when naive Th cells were sorted and stimulated under the same condition (Fig. 3*C*). This unexpected finding seems to be derived from the fact that most of the c-Maf Tg Th cells from the spleen demonstrate an effector-memory phenotype ($CD62L^{low}$ $CD44^{high}$, Fig. 3*D*). These results suggest that c-Maf does not play an essential role in the early differentiation of Th17 cells but rather in the development and/or maintenance of memory Th cells.

Analysis of WT Memory Phenotype Th Cells—The above findings on Tg Th cells prompted us to analyze WT memory Th cells. Under specific pathogen-free conditions, nearly 80% of the Th cells from the spleens of WT mice demonstrated the naive phenotype ($CD62L^{high}$ $CD44^{low}$, Fig. 4*A*, *left panel*). To facilitate the analysis of memory phenotype WT Th cells, we utilized the system of homeostatic expansion; when naive T cells are transferred into lymphopenic mice, they proliferate vigorously and acquire the memory phenotype (27). Thus, we transferred WT Th cells into Rag-2-deficient mice. In 4 weeks, most of the splenic Th cells from the recipient mice acquired an effector-memory phenotype ($CD62L^{low}$ $CD44^{high}$, Fig. 4*A*, *right panel*). When compared with WT naive Th cells, these cells expressed significantly higher mRNA levels of *Maf* and *Il23r* (Fig. 4*B*). Similar to the results in Fig. 3, these cells also expressed higher levels of *Il17a* and *Ifng* mRNAs, but not *Il4* mRNA (Fig. 4*C*). Consistent with the data, flow cytometric analysis revealed more IFN-γ-positive and IL-17-positive cells than WT naive cells (Fig. 4*D* and data not shown). Interestingly, an IFN-γ/IL-17 double-positive population was evident (IL-17 single-positive cells and IFN-γ/IL-17 double-positive cells were present at similar levels). On the other hand, IL-4-positive cells were scarcely observed.

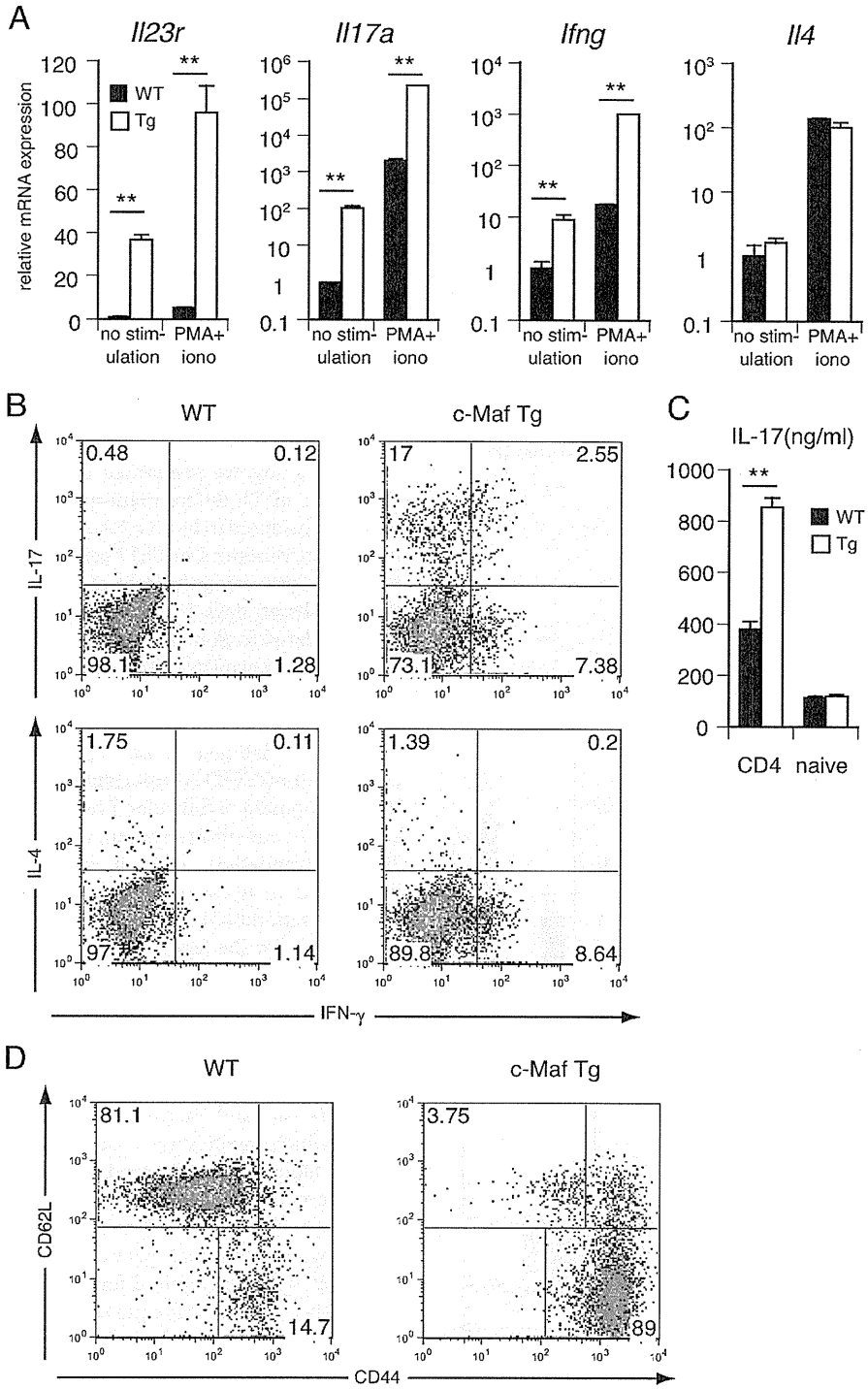

FIGURE 3. ***Ex vivo* gain-of-function analysis of c-Maf.** *A*, comparison between freshly isolated WT (*black bars*) and littermate c-Maf Tg (*white bars*) Th cells of the expression of Th differentiation markers. *B*, flow cytometric analysis of Th cells from c-Maf Tg and littermate WT mice. c-Maf Tg Th cells express more IL-17 and IFN-γ, but not IL-4, than control cells. *C*, IL-17 production from WT (*black bars*) and c-Maf Tg (*white bars*) Th cells or $CD62L^{high}$ naive Th cells stimulated *in vitro* under Th17 differentiation condition for 2 days. IL-17 released into the culture supernatant was detected by ELISA. *D*, flow cytometric analysis of splenocytes from WT and c-Maf Tg mice gated on $CD4^+$ population. Single-cell suspensions of splenocytes were stained with anti-CD4-FITC, anti-CD44-PE, and anti-CD62L-APC mAbs and analyzed by FACSCanto. 7-Amino-Actinomycin D was used to separate dead cells. Similar results were obtained in three independent experiments. **, $p < 0.01$.

Ex Vivo Analysis of c-Maf-deficient Th Cells—As c-Maf deficient mice are embryonic lethal, we generated bone marrow chimeras by injecting $Maf^{-/-}$ fetal liver cells containing hematopoietic stem cells into irradiated Rag-2-deficient mice. Six weeks later, the donor mice were sacrificed, and flow cytometric analysis of splenocytes was performed. The ratio of effector-

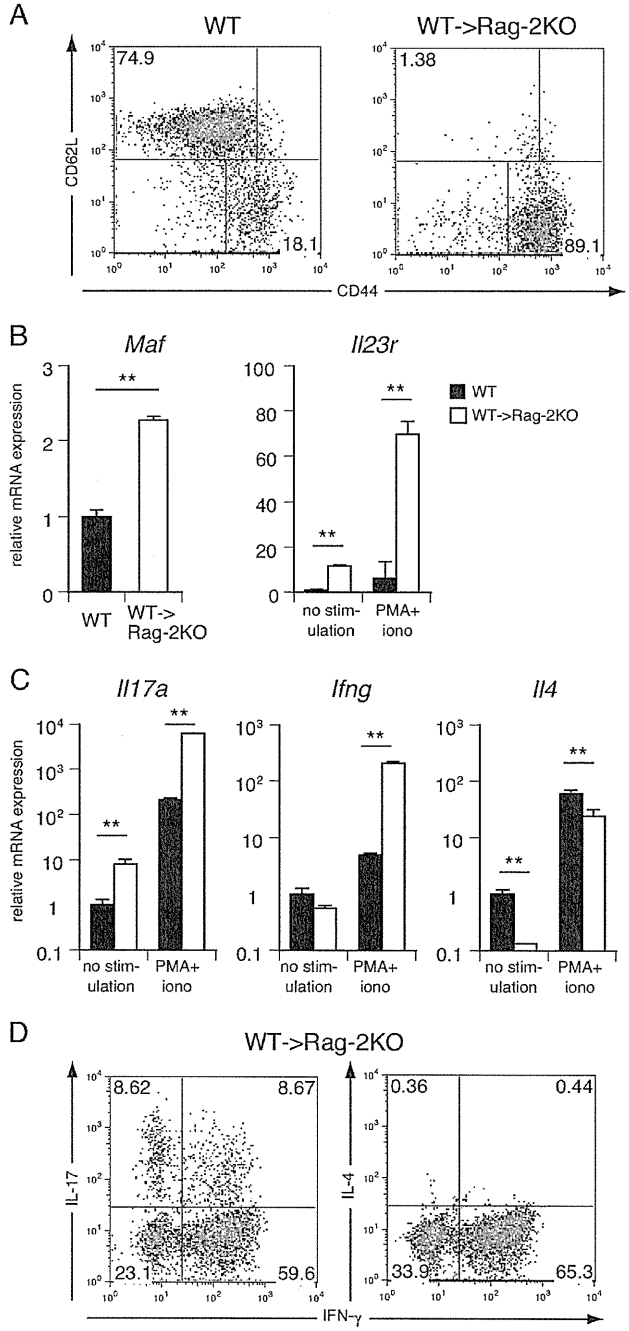

FIGURE 4. **Analysis of WT naive Th cells and memory Th cells derived from Rag-2-deficient mice transferred with WT Th cells.** *A*, flow cytometry of WT splenocytes and splenocytes from Rag-2-deficient mice transferred with WT Th cells (10^6/mouse) 4 weeks before analysis. An analysis similar to that shown in Fig. 3*D* was performed. Note that nearly 90% of the $CD4^+$ cells became $CD44^{high}$ $CD62L^{low}$, leaving only about 1% $CD44^{low}$ $CD62L^{high}$ cells. *B* and *C*, qRT-PCR analysis of the expressions of *Maf* and *Il23r* in naive (*black bars*) and memory (*white bars*) Th cells (*B*) and those of *Il17a*, *Ifng*, and *Il4* (*C*). *D*, flow cytometric analysis of memory phenotype Th cells. IL-17-positive and IFN-γ-positive populations were evident, but IL-4-positive one was not. Data represent three independent experiments. *PMA*, phorbol 12-myristate 13-acetate; *iono*, ionomycin. **, $p < 0.01$.

memory phenotype Th cells ($CD62L^{low}$ $CD44^{high}$) was not significantly different from that of WT Th cells (data not shown). As $Maf^{-/-}$-naive Th cells were shown to have the capacity to differentiate into Th17 cells *in vitro* (28), we decided to analyze the memory-phenotype c-Maf-deficient Th cells by transferring sorted splenic Th cells to Rag-2-deficient mice as in the experiment whose results are shown in Fig. 4 (Fig. 5*A*). In 4 weeks, most of the transferred Th cells acquired an effector-memory phenotype, and these cells were analyzed by qRT-PCR for the expressions of cytokines and *Il23r*. As expected, *Il23r*, *Il17a*, and *Ifng* expression levels were significantly lower in these cells than in the control WT cells. The expression level of *Il21*, which was reported to be a transcriptional target of c-Maf, was also lower (Fig. 5*B*).

DISCUSSION

In this study, we performed transcriptome analysis during the course of Th differentiation and unexpectedly found that c-Maf, considered to be a Th2-type transcription factor, is more prominently induced in Th17 cells than in Th2 cell. Moreover, factor analysis using the data of Th1-, Th2- and Th17-conditioned cells on days 1 and 3 demonstrated that *Maf* is more closely related to *Rorc* than *Rora* is to *Rorc*, at least in terms of the expression profiles in Th cells. As both RORγ and RORα are considered to play essential roles in Th17 differentiation (16), it occurred to us that c-Maf may also play an important role in Th17 cells. Bauquet *et al.* reported that inducible T cell costimulator (ICOS) is important for the expression of c-Maf in the development of follicular T helper cells (Tfh cells) and Th17 cells (28). In our culture system, we did not use ICOS-ligand for Th-cell stimulation. Thus, it is obvious that c-Maf can be induced in an ICOS-independent manner, probably through Stat3 activation by IL-6 (24).

As shown in the factor analysis results (Fig. 1*B*), *Maf*, *Rorc* and *Rora* were all high in Factor 2 but low in Factor 1. In contrast, *Gata3*, which encodes the master regulator transcription factor of Th2 cells, was very high in Factor 1 but low in Factor 2, and so was *Stat5a*, which is implicated in Th2 differentiation (29, 30). From these data, we may safely call Factor 1 "a Th2-related factor" and Factor 2 "a Th17-related factor". Indeed, *Tbx21*, which encodes the master regulator of Th1 cells, T-bet, was not high in either Factor 1 or Factor 2 and was positioned near the coordinate origin. Thus, these transcription factor groups specific to Th1, Th2 and Th17 cells are separately placed on the two-dimensional space defined by Factors 1 and 2.

IL-23R, which is required for the expansion of Th17 cells, is among the candidates for the transcriptional targets of c-Maf. Indeed, the promoter analysis revealed that MARE located in the 5′-prime lesion of *Il23r* is important for the luciferase activity induced by c-Maf overexpression, indicating that IL-23R is a direct target of c-Maf (Fig. 2*C*). IL-21 (28) and IL-10 (31) have also recently been reported to be targets of c-Maf in the context of Th17 differentiation. The analysis of c-Maf Tg mice, however, demonstrated that the overexpression of c-Maf did not seem to accelerate the early stage of Th17 differentiation (Fig. 3*C*). This finding is consistent with that of Bauquet *et al.*, in which c-Maf-deficient Th cells were capable of producing IL-17, although at a lower level (28). Instead, the significant

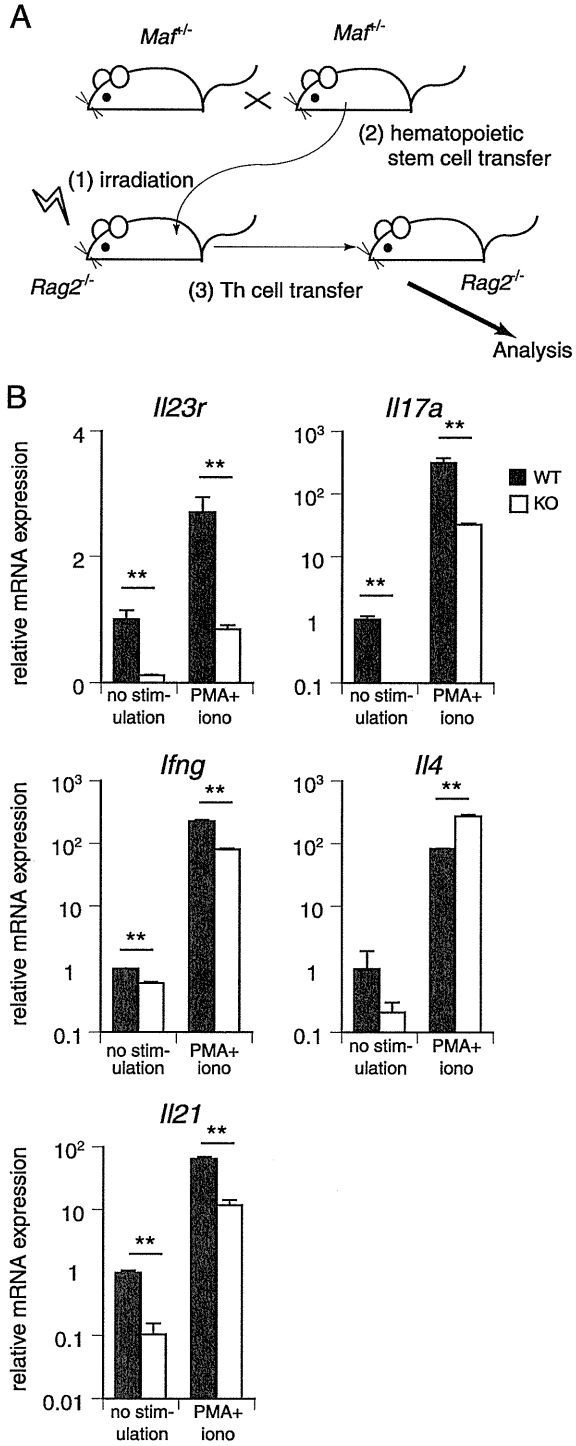

FIGURE 5. ***Ex vivo* loss-of-function analysis of c-Maf utilizing bone marrow chimera.** *A*, schematic diagram of producing bone marrow chimera and successive transfer of Th cells into Rag-2 knock-out mice. *B*, qRT-PCR analysis of the expressions of *Il23r*, *Il17a*, *Ifng*, *Il4*, and *Il21* in *Maf*$^{-/-}$ memory Th cells and control cells. Data represent three independent experiments. *PMA+ iono*, phorbol 12-myristate 13-acetate + ionomycin. **, $p < 0.01$.

deviation of Th cells toward the memory phenotype was observed in the Tg mice, suggesting that c-Maf may play a role in the development and/or maintenance of memory Th cells. The fact that WT mouse memory Th cells express higher mRNA levels of not only *Maf*, *Il23r* and *Il17a* but also *Ifng* than non-memory cells suggests that c-Maf indeed plays a role in memory Th17 and Th1 cells (Fig. 4*B* and *C*). In the earliest studies of Th cells and IL-17, it was memory Th cell that was shown to mainly produce the cytokine (32) particularly in response to IL-23 (33). It was not until the discovery of Th17 cells that these IL-17-producing cells were considered to be distinct from Th1 cells. Recently, however, Th cells that produce both IFN-γ and IL-17 have been gathering attention particularly in the context of inflammation, making the difference between Th1 and Th17 subsets less clear again (34–36). Although the relationship between memory Th cells and Th17 cells differentiated *in vitro* seems to be close in that both subsets express IL-23R, we have yet to determine whether Th17 cells differentiated *in vitro* are indeed the precursors of memory Th cells *in vivo*. If that is the case, c-Maf, which is expressed highly in both *de novo* Th17 cells and memory Th cell, may be a transcription factor that mediates the differentiation of the former into the latter.

In regard to this point, it is interesting that an IFN-γ/IL-17 double-positive population was evident in memory phenotype Th cells (Fig. 4*D*), which was not so apparent in Maf Tg cells. It is likely that the forced expression of c-Maf is sufficient for the expression of surface markers of memory Th cells, but not sufficient for the differentiation of IFN-γ/IL-17 double-positive Th cells.

The homeostatic expansion and induction of memory phenotype Th cells are important in a variety of clinical situations, such as during immunosuppressive therapy or chemotherapy. There is little doubt that the expansion of memory phenotype Th cells plays an important role in the defense against numerous pathogens, for example, those residing in the gut. At the same time, such expansion also bears the risk of autoinflammation, causing damage to self tissues. It has been shown that adoptive transfer of naive Th cells into lymphopenic hosts induces inflammatory bowel disease, which can be prevented by cotransfer of regulatory T (Treg) cells (37). Th1 response is implicated in the pathogenesis, whereas the role Th17 cells play in this disease model is still controversial (38). In either case, Treg cells seem to be essential for controlling the excessive response of homeostatically expanding Th cells.

It was unexpected that c-Maf Tg Th cells did not produce more IL-4 than WT cells (Fig. 3*A* and *B*), although c-Maf was reported to play an important role in IL-4 production (39). Consistently, the expression of *Il4* was not reduced in *Maf*$^{-/-}$ Th cells than in WT cells, either (Fig. 5*B*). These results may be explained by the fact that the Th1 cytokine IFN-γ strongly inhibits Th2 differentiation (40). Consistently, c-Maf Tg CD62L^{low} Th cells caused Th1-mediated colitis in Rag-2-deficient mice whereas WT CD62L^{low} Th cells did not (41). Thus, it is possible that the overexpression of c-Maf tips the balance of Th response toward Th1 rather than Th2 type under a neutral condition. In fact, c-Maf Tg Th cells produce more IL-4 than WT cells when cultured under a Th2 condition in the presence

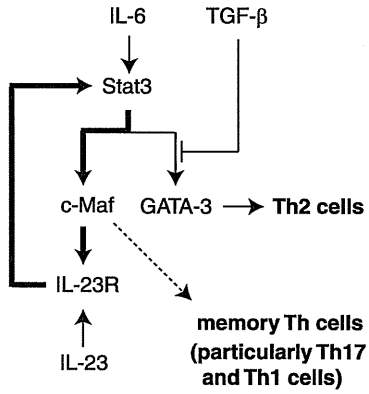

FIGURE 6. **Schematic diagram of Th cell differentiation.** IL-6 induces both c-Maf and GATA-3 via Stat3 phosphorylation and activation. GATA-3 expression can lead to Th2 differentiation, but this route is blocked in the presence of TGF-β, which inhibits GATA-3 expression. c-Maf induces IL-23R, and then IL-23 signaling activates Stat3, constituting a positive feedback loop (*boldface lines*). Although this loop does not seem to be essential to early Th17 differentiation, it may play an important role in the development and/or maintenance of memory Th cells, particularly memory Th17 cells.

of IL-4 and anti-IFN-γ antibody (in other words, in the absence of IFN-γ, data not shown). A schematic of Th cell differentiation is shown in Fig. 6; IL-6 induces c-Maf expression via Stat3 phosphorylation and is particularly important for the induction of IL-23R, which in turn augments Stat3 phosphorylation, constituting a novel positive feedback loop that leads to the differentiation of memory Th17 cells. On the other hand, TGF-β is likely involved in the inhibition of GATA-3 induction by IL-6, thereby blocking the pathway for Th cells to differentiate into Th2 cells.

c-Maf has also been implicated in the differentiation of other Th cell types, including Tfh cells (28) and regulatory type 1 (Tr1) cells (42). Our study indicates that this versatile transcription factor is also involved in the development and/or maintenance of memory Th (particularly Th17) cells. Clarification of the mechanisms of memory Th cell development in the context of c-Maf induction would be beneficial in the understanding of pathophysiology of various autoimmune inflammatory diseases.

Acknowledgments—We are grateful to S. Kano, M. Asagiri, H. J. Gober, and U. Sato for fruitful discussion and critical reading of the manuscript. We also thank Y. Meguro, M. Hamada, Y. Yamada, A. Kawano, and K. Watanabe for technical advice and assistance.

REFERENCES

1. Harrington, L. E., Hatton, R. D., Mangan, P. R., Turner, H., Murphy, T. L., Murphy, K. M., and Weaver, C. T. (2005) *Nat. Immunol.* **6,** 1123–1132
2. Park, H., Li, Z., Yang, X. O., Chang, S. H., Nurieva, R., Wang, Y. H., Wang, Y., Hood, L., Zhu, Z., Tian, Q., and Dong, C. (2005) *Nat. Immunol.* **6,** 1133–1141
3. Bettelli, E., Oukka, M., and Kuchroo, V. K. (2007) *Nat. Immunol.* **8,** 345–350
4. Steinman, L. (2007) *Nat. Med.* **13,** 139–145
5. Veldhoen, M., Hocking, R. J., Atkins, C. J., Locksley, R. M., and Stockinger, B. (2006) *Immunity* **24,** 179–189
6. Bettelli, E., Carrier, Y., Gao, W., Korn, T., Strom, T. B., Oukka, M., Weiner, H. L., and Kuchroo, V. K. (2006) *Nature* **441,** 235–238
7. Mangan, P. R., Harrington, L. E., O'Quinn, D. B., Helms, W. S., Bullard, D. C., Elson, C. O., Hatton, R. D., Wahl, S. M., Schoeb, T. R., and Weaver, C. T. (2006) *Nature* **441,** 231–234
8. Wilson, N. J., Boniface, K., Chan, J. R., McKenzie, B. S., Blumenschein, W. M., Mattson, J. D., Basham, B., Smith, K., Chen, T., Morel, F., Lecron, J. C., Kastelein, R. A., Cua, D. J., McClanahan, T. K., Bowman, E. P., and de Waal Malefyt, R. (2007) *Nat. Immunol.* **8,** 950–957
9. Manel, N., Unutmaz, D., and Littman, D. R. (2008) *Nat. Immunol.* **9,** 641–649
10. Volpe, E., Servant, N., Zollinger, R., Bogiatzi, S. I., Hupé, P., Barillot, E., and Soumelis, V. (2008) *Nat. Immunol.* **9,** 650–657
11. McGeachy, M. J., Bak-Jensen, K. S., Chen, Y., Tato, C. M., Blumenschein, W., McClanahan, T., and Cua, D. J. (2007) *Nat. Immunol.* **8,** 1390–1397
12. Ghoreschi, K., Laurence, A., Yang, X. P., Tato, C. M., McGeachy, M. J., Konkel, J. E., Ramos, H. L., Wei, L., Davidson, T. S., Bouladoux, N., Grainger, J. R., Chen, Q., Kanno, Y., Watford, W. T., Sun, H. W., Eberl, G., Shevach, E. M., Belkaid, Y., Cua, D. J., Chen, W., and O'Shea, J. J. (2010) *Nature* **467,** 967–971
13. Nishihara, M., Ogura, H., Ueda, N., Tsuruoka, M., Kitabayashi, C., Tsuji, F., Aono, H., Ishihara, K., Huseby, E., Betz, U. A., Murakami, M., and Hirano, T. (2007) *Int. Immunol.* **19,** 695–702
14. Yang, X. O., Panopoulos, A. D., Nurieva, R., Chang, S. H., Wang, D., Watowich, S. S., and Dong, C. (2007) *J. Biol. Chem.* **282,** 9358–9363
15. Ivanov, II, McKenzie, B. S., Zhou, L., Tadokoro, C. E., Lepelley, A., Lafaille, J. J., Cua, D. J., and Littman, D. R. (2006) *Cell* **126,** 1121–1133
16. Yang, X. O., Pappu, B. P., Nurieva, R., Akimzhanov, A., Kang, H. S., Chung, Y., Ma, L., Shah, B., Panopoulos, A. D., Schluns, K. S., Watowich, S. S., Tian, Q., Jetten, A. M., and Dong, C. (2008) *Immunity* **28,** 29–39
17. Morito, N., Yoh, K., Fujioka, Y., Nakano, T., Shimohata, H., Hashimoto, Y., Yamada, A., Maeda, A., Matsuno, F., Hata, H., Suzuki, A., Imagawa, S., Mitsuya, H., Esumi, H., Koyama, A., Yamamoto, M., Mori, N., and Takahashi, S. (2006) *Cancer Res.* **66,** 812–819
18. Imai, Y., Matsushima, Y., Sugimura, T., and Terada, M. (1991) *Nucleic Acids Res.* **19,** 2785
19. Sato, K., Hida, S., Takayanagi, H., Yokochi, T., Kayagaki, N., Takeda, K., Yagita, H., Okumura, K., Tanaka, N., Taniguchi, T., and Ogasawara, K. (2001) *Eur. J. Immunol.* **31,** 3138–3146
20. Kim, Y., Sato, K., Asagiri, M., Morita, I., Soma, K., and Takayanagi, H. (2005) *J. Biol. Chem.* **280,** 32905–32913
21. Kajihara, M., Sone, H., Amemiya, M., Katoh, Y., Isogai, M., Shimano, H., Yamada, N., and Takahashi, S. (2003) *Biochem. Biophys. Res. Commun.* **312,** 831–842
22. Ko, L. J., Yamamoto, M., Leonard, M. W., George, K. M., Ting, P., and Engel, J. D. (1991) *Mol. Cell Biol.* **11,** 2778–2784
23. Ho, I. C., Hodge, M. R., Rooney, J. W., and Glimcher, L. H. (1996) *Cell* **85,** 973–983
24. Yang, Y., Ochando, J., Yopp, A., Bromberg, J. S., and Ding, Y. (2005) *J. Immunol.* **174,** 2720–2729
25. Gorelik, L., Fields, P. E., and Flavell, R. A. (2000) *J. Immunol.* **165,** 4773–4777
26. Yamamoto, T., Kyo, M., Kamiya, T., Tanaka, T., Engel, J. D., Motohashi, H., and Yamamoto, M. (2006) *Genes Cells* **11,** 575–591
27. Min, B., Yamane, H., Hu-Li, J., and Paul, W. E. (2005) *J. Immunol.* **174,** 6039–6044
28. Bauquet, A. T., Jin, H., Paterson, A. M., Mitsdoerffer, M., Ho, I. C., Sharpe, A. H., and Kuchroo, V. K. (2009) *Nat. Immunol.* **10,** 167–175
29. Zhu, Y., Chen, L., Huang, Z., Alkan, S., Bunting, K. D., Wen, R., Wang, D., and Huang, H. (2004) *J. Immunol.* **173,** 2918–2922
30. Takatori, H., Nakajima, H., Hirose, K., Kagami, S., Tamachi, T., Suto, A., Suzuki, K., Saito, Y., and Iwamoto, I. (2005) *J. Immunol.* **174,** 3734–3740
31. Xu, J., Yang, Y., Qiu, G., Lal, G., Wu, Z., Levy, D. E., Ochando, J. C., Bromberg, J. S., and Ding, Y. (2009) *J. Immunol.* **182,** 6226–6236
32. Shin, H. C., Benbernou, N., Esnault, S., and Guenounou, M. (1999) *Cytokine* **11,** 257–266
33. Aggarwal, S., Ghilardi, N., Xie, M. H., de Sauvage, F. J., and Gurney, A. L. (2003) *J. Biol. Chem.* **278,** 1910–1914
34. Boniface, K., Blumenschein, W. M., Brovont-Porth, K., McGeachy, M. J., Basham, B., Desai, B., Pierce, R., McClanahan, T. K., Sadekova, S., and de

Waal Malefyt, R. (2010) *J. Immunol.* **185,** 679–687
35. Acosta-Rodriguez, E. V., Rivino, L., Geginat, J., Jarrossay, D., Gattorno, M., Lanzavecchia, A., Sallusto, F., and Napolitani, G. (2007) *Nat. Immunol.* **8,** 639–646
36. Kebir, H., Ifergan, I., Alvarez, J. I., Bernard, M., Poirier, J., Arbour, N., Duquette, P., and Prat, A. (2009) *Ann. Neurol.* **66,** 390–402
37. Izcue, A., Coombes, J. L., and Powrie, F. (2006) *Immunol. Rev.* **212,** 256–271
38. O'Connor, W., Jr., Kamanaka, M., Booth, C. J., Town, T., Nakae, S., Iwakura, Y., Kolls, J. K., and Flavell, R. A. (2009) *Nat. Immunol.* **10,** 603–609
39. Kim, J. I., Ho, I. C., Grusby, M. J., and Glimcher, L. H. (1999) *Immunity* **10,** 745–751
40. Gajewski, T. F., and Fitch, F. W. (1988) *J. Immunol.* **140,** 4245–4252
41. Weigmann, B., Nemetz, A., Becker, C., Schmidt, J., Strand, D., Lehr, H. A., Galle, P. R., Ho, I. C., and Neurath, M. F. (2004) *J. Immunol.* **173,** 3446–3455
42. Pot, C., Jin, H., Awasthi, A., Liu, S. M., Lai, C. Y., Madan, R., Sharpe, A. H., Karp, C. L., Miaw, S. C., Ho, I. C., and Kuchroo, V. K. (2009) *J. Immunol.* **183,** 797–801

Geranylgeranyl-pyrophosphate regulates secretion of pentraxin 3 and monocyte chemoattractant protein-1 from rheumatoid fibroblast-like synoviocytes in distinct manners

K. Yokota, F. Miyoshi, K. Sato, Y. Asanuma, Y. Akiyama, T. Mimura

Department of Rheumatology and Applied Immunology, Faculty of Medicine, Saitama Medical University, Saitama, Japan.

Abstract

Objectives

We previously reported that 10 mg/day of simvastatin significantly reduced clinical scores of rheumatoid arthritis (RA) in active RA patients with hypercholesterolemia. In this study, we have investigated the mechanism by which simvastatin inhibits the production of the mediators of inflammation, such as pentraxin 3 (PTX3) and monocyte chemoattractant protein-1 (MCP-1), from fibroblast-like synoviocytes (FLS) derived from patients with RA.

Methods

FLS from RA patients were cultured with 0-10 μM simvastatin for 24 h. ELISA and real-time PCR were used to quantitate the protein level and the mRNA level of PTX3 and MCP-1, respectively.

Results

Simvastatin both reduced the secretion of PTX3 and MCP-1 in FLS cultures and inhibited their mRNA expression in these cells. The effects of simvastatin were all completely reversed in the presence of mevalonic acid or geranylgeranyl-pyrophosphate, but not in the presence of farnesyl-pyrophosphate. The geranylgeranyl transferase inhibitor GGTI-298 and the Rho kinase inhibitor Y-27632 inhibited the production of PTX3 but not of MCP-1.

Conclusions

Although simvastatin inhibited the production of PTX3 and MCP-1 in RA FLS, the mechanisms were quite different. It inhibits PTX3 production in a Rho-dependent manner but MCP-1 production in a Rho-independent manner. These results shed light on novel aspects of the anti-inflammatory mechanisms of simvastatin and may prove its important role in the treatment of rheumatic diseases.

Key words

rheumatoid arthritis, fibroblast-like synoviocytes, 3-hydroxy-3-methylglutaryl co-enzyme A reductase inibitor, pentraxin 3, monocyte chemoattractant protein-1, small G protein

Kazuhiro Yokota, MD, PhD
Fumihiko Miyoshi, PhD
Kojiro Sato, MD, PhD
Yu Asanuma, MD, PhD
Yuji Akiyama, MD, PhD
Toshihide Mimura, MD, PhD

This study was partially supported by a grant from Ochiai Memorial award 2008.

Please address correspondence and reprint requests to:
Dr Toshihide Mimura
Department of Rheumatology and Applied Immunology,
Faculty of Medicine,
Saitama Medical University,
38 Morohongo, Moroyama-machi,
Iruma-gun, Saitama 350-0495,
Japan.
E-mail: toshim@saitama-med.ac.jp

Received on April 20, 2010; accepted in revised form on October 11, 2010.

Competing interests: none declared.

Introduction

Pentraxins are a family of evolutionarily conserved, soluble and multifunctional pattern recognition proteins characterised by a cyclic multimeric structure (1). Pentraxins are divided into two groups: short pentraxins and long pentraxins. The short pentraxins consist of C-reactive protein (CRP) and serum amyloid P (SAP) (2). The prototype protein in the long pentraxin group is pentraxin 3 (PTX3). PTX3 has been suggested to play important roles in innate resistance to pathogens, the regulation of inflammatory reactions and the clearance of apoptotic cells (3). While short pentraxins are produced mainly in the liver (4), PTX3 is made by diverse types of cells, including endothelial cells, macrophages and fibroblasts, in response to inflammatory signals (1). Recently, PTX3 levels have been shown to be increased in synovial fluid and synovial tissue from patients with rheumatoid arthritis (RA) (5).

The 3-hydroxyl-3-methylglutaryl-CoA (HMG-CoA) reductase inhibitors, statins, have shown to reduce both morbidity and mortality in many clinical trials (6, 7). Many studies have also demonstrated a wide range of their effects on cells and tissues involved in inflammation and/or autoimmunity. For example, statins attenuated the expression of interferon-γ-induced class II major histocompatibility complex molecules, via the class II transactivator protein, in a variety of cells, such as endothelial cells and monocytes/macrophages, and thus to inhibit T cell activation (8). It has been reported that lovastatin and simvastatin inhibit the interactions between leukocyte function-associated antigen 1 (LFA-1) and intercellular adhesion molecule 1 by binding to a specific recognition site on LFA-1, which is independent of their HMG-CoA reductase activity (9).

HMG-CoA reductase, a target enzyme of statins, catalyses the conversion of HMG-CoA to mevalonic acid (MVA) (10). Inhibiting MVA synthesis results in a reduced pool of isoprenoids, such as geranylgeranyl-pyrophosphate (GGPP) and farnesyl-pyrophosphate (FPP), which are involved in the post-translational modification of small GTP-binding proteins, including members of the Ras and Rho families, *i.e.*, Rho, Rac and Cdc42. Thus, MVA is considered to antagonise the whole effects of statins. On the other hand, FPP rescues the activation of Ras in the presence of statins. GGPP rescues the activation of Rho family members by way of geranylgeranyl transferase type I (GGTase I), which is inhibited by GGTI-298.

Prenylation of small GTP-binding proteins with farnesyl or geranylgeranyl groups is required for their localisation within cell membranes and hence for their function (11). Ras is farnesylated with FPP, and Rho family members are geranylgeranylated with GGPP and act as pivotal regulators of several signalling networks affecting actin cytoskeleton dynamics, transcriptional regulation, cell cycle progression and membrane trafficking (11). The key enzyme of post-translational modifications of the Rho family is GGTase I (11), which can be selectively inhibited by peptidomimetic inhibitors, such as GGTI-298 (12). When cells are stimulated, geranylgeranylated Rho binds to specific effectors to exert its biological functions, which can be specifically inhibited by Y-27632, a Rho kinase inhibitor (13).

We have previously shown that simvastatin significantly improved clinical indicators in RA patients with active disease (14, 15). We have also reported recently that pharmacological concentrations of simvastatin inhibit production of interleukin 6 (IL-6) and IL-8 and cell proliferation induced by tumour necrosis factor-α (TNF-α) in fibroblast-like synoviocytes (FLS) from patients with RA (16) and that high concentration simvastatin induces apoptosis in FLS from patients with RA (17).

In the present study, we have investigated the effect of simvastatin on the production of PTX3 and compared the mechanism with that on the production of monocyte chemoattractant protein-1 (MCP-1) by FLS derived from patients with RA.

Materials and methods

Reagents

Simvastatin was kindly provided by Merck & Co. Inc. (Rahway, NJ, USA).

A 10 mM stock solution was prepared as previously described (16). Briefly, 4 mg simvastatin was dissolved in 100 μl of ethanol and 150 μl of 0.1 N NaOH and incubated at 50°C for 2 h; the pH was adjusted to 7.0 and the volume to 1.0 ml. A control solution without simvastatin was prepared in the same way. Other chemicals and materials were purchased from the following sources: RPMI 1640 medium, fetal calf serum (FCS), penicillin and streptomycin were from Invitrogen (Carlsbad, CA, USA); trypsin/EDTA, collagenase, hyaluronidase, mevalonic acid (MVA), farnesyl-pyrophosphate (FPP) and geranylgeranyl-pyrophosphate (GGPP) were from Sigma (St. Louis, MO, USA); GGTI-298 and Y-27632 were from Calbiochem (Schwalbach, Germany). We previously used GGTI-298 at the concentration of 5 to 15 μM and Y-27632 at 3 to 10 μM (17). We therefore originally chose similar concentrations. Y-27632, however, did not affect the production of MCP-1 and PTX-3 at the chosen concentrations. We therefore decided to use Y-27632 at higher concentrations (30-60 μM). Total RNA samples from cultured FLS were purified using the RNeasy mini-kit from QIAGEN GmbH (Hilden, Germany). Taqman reverse transcription reagents, Taqman universal PCR master mix, TaqMan Gene Expression Assays for PTX3 and Taqman Pre-Developed Assay Reagents for MCP-1 and glyceraldehydes-3-phosphate dehydrogenase (GAPDH) were from Applied Biosystems (Foster City, CA, USA). ELISA kits for PTX3 and MCP-1 were purchased from Perseus Proteomics Inc. (Tokyo, Japan) and GE Healthcare (Buckinghamshire, UK), respectively.

Preparation and culture of FLS

Synovial tissues were obtained from 8 RA and 3 osteoarthritis (OA) patients who underwent joint replacement at Saitama Medical University. The patients with RA fulfilled the revised 1987 American College of Rheumatology differentiation criteria. A written informed consent, approved by the ethics committee at Saitama Medical University, was obtained from each patient, prior to the experiment. FLS were isolated and cultured as previously described (16). Briefly, synovial tissue was minced into small pieces and shaken for 2 h at 37°C in RPMI 1640 containing 0.15 mg/ml collagenase and 0.04% hyaluronidase. After removing tissue debris using a 70 μm nylon mesh, the cells were cultured in RPMI 1640 containing 10% FCS, 100 U/ml penicillin and 100 μg/ml streptomycin in a humidified 5% CO_2 incubator at 37°C. Non-adherent cells were removed the next day and adherent cells were maintained as FLS. Sub-confluent cells were sub-cultured using trypsin/EDTA and plated in 24-well plates or 100-mm culture dishes and again grown to sub-confluence. Experiments were carried out in RPMI 1640 containing 1% FCS using FLS from passages three to seven in a humidified 5% CO_2 incubator at 37°C.

Quantitative PCR

Total RNA was extracted from FLS, using RNeasy Mini Kits according to the manufacturer's instructions. Total RNA samples were reverse transcribed using Taqman Reverse Transcription Reagents. The mRNA expression level was determined using a Taqman PCR system and an ABI PRISM 7000 Sequence Detection System (Applied Biosystems). PTX3 and MCP-1 mRNAs were detected using TaqMan Gene Expression Assays and Taqman Pre-Developed Assay Reagent kits, respectively. GAPDH was amplified simultaneously and used for standardisation. PCR reactions consisted of 25 μl 2x Taqman Universal PCR Master Mix, 2.5 μl 20x target primers and probe, 2.5 μl 20x control primers and probe and 300 ng cDNA, and were made up to 50 μl with RNase-free water. The conditions for quantitative PCR were; 95°C for 10 min, followed by 40 cycles of 2-step PCR, including denaturation at 95°C for 15 s and annealing/extension at 60°C for 1 min. For quantitative mRNA analysis for PTX3 and MCP-1, changes in the reporter fluorescence from each reaction well were evaluated. For each gene, the threshold cycle (Ct) was defined as the PCR cycle at which fluorescence rose above baseline. The difference between the threshold cycle of the target gene and that of the control GAPDH gene gave the standardised expression level, ΔCt. The difference between ΔCt values for nontreated and simvastatin-treated FLS gave the ΔΔCt value, which was used to calculate relative expression level in simvastatin-treated FLS as $2^{-\Delta\Delta Ct}$. The expression level of each gene was interpreted as fold-increase in simvastatin-treated FLS compared with that in nontreated controls (16).

ELISA for PTX3 and MCP-1

The detection of PTX3 and MCP-1 proteins in cell supernatants was performed with PTX3 and MCP-1 ELISA kits according to the manufacturer's instructions.

Statistical analysis

All data were expressed as means ± standard error (SEM). Statistical analysis used the Mann-Whitney U-test with p-values <0.05 considered as significant.

Results

Inhibitory effects of simvastatin on PTX3 production in FLS

As shown in Figure 1A, the levels of PTX3 secreted by RA FLS after 24 h-culture in the absence of simvastatin were significantly higher than those with OA. When FLS from RA patients were incubated for 24 h with simvastatin, PTX3 in culture supernatants was reduced significantly, to 70.0±2.0% of control in the presence of 1.0 μM simvastatin and 62.0±6.7% of control in the presence of 10 μM simvastatin (Fig. 1B). The expression of PTX3 mRNA was also reduced in cultures treated with simvastatin, to 62.3±11.0%, 38.8±5.0% and 14.3±1.2%, compared with control, in the presence of 0.1 μM, 1.0 μM and 10 μM simvastatin, respectively (Fig. 1C).

MVA and GGPP restore the production of PTX3 in FLS in the presence of simvastatin

As shown in Figure 2A, the inhibitory effect of 1.0 μM simvastatin on PTX3 production in RA FLS was suppressed when the cells were simultaneously treated with 100 μM MVA or 10 μM GGPP, but unaffected with FPP. MVA, GGPP and FPP had minimal effects

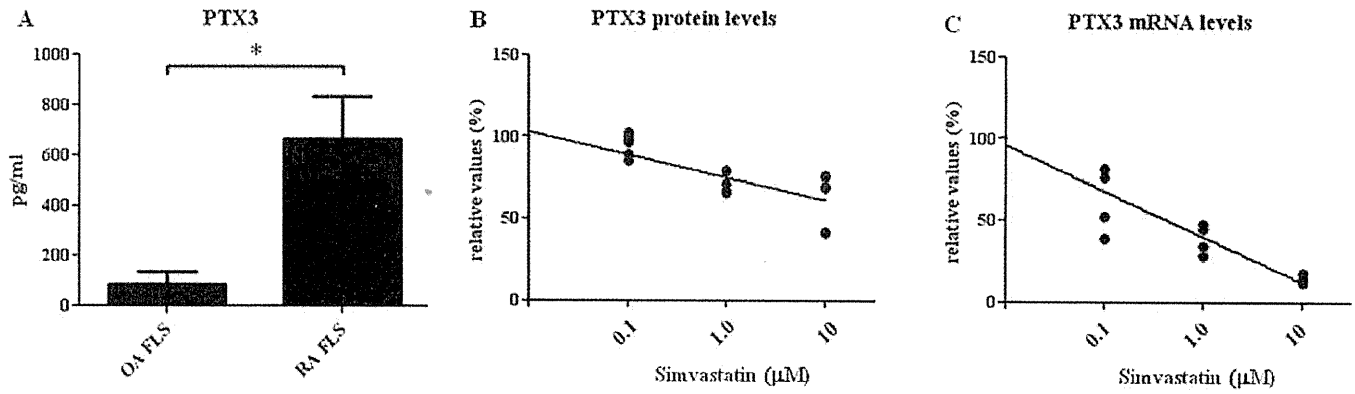

Fig. 1. RA FLS specifically produced PTX3, which was suppressed by simvastatin.
A. FLS from patients with RA or OA were incubated without simvastatin for 24 h. PTX3 levels in culture supernatants were determined by ELISA. Data are expressed as means ± SEM of duplicate experiments (n=6); $^{*}p<0.05$ versus control. **B, C.** The expression of PTX3 was reduced by simvastatin in a dose-dependent manner both at the protein level (**B**, n=6) and at the mRNA level (**C**, n=4). FLS from RA patients were incubated with 0.1–10 μM simvastatin for 24 h. Data shown are values relative to control cells cultured in the absence of simvastatin. Tendency lines are also shown.

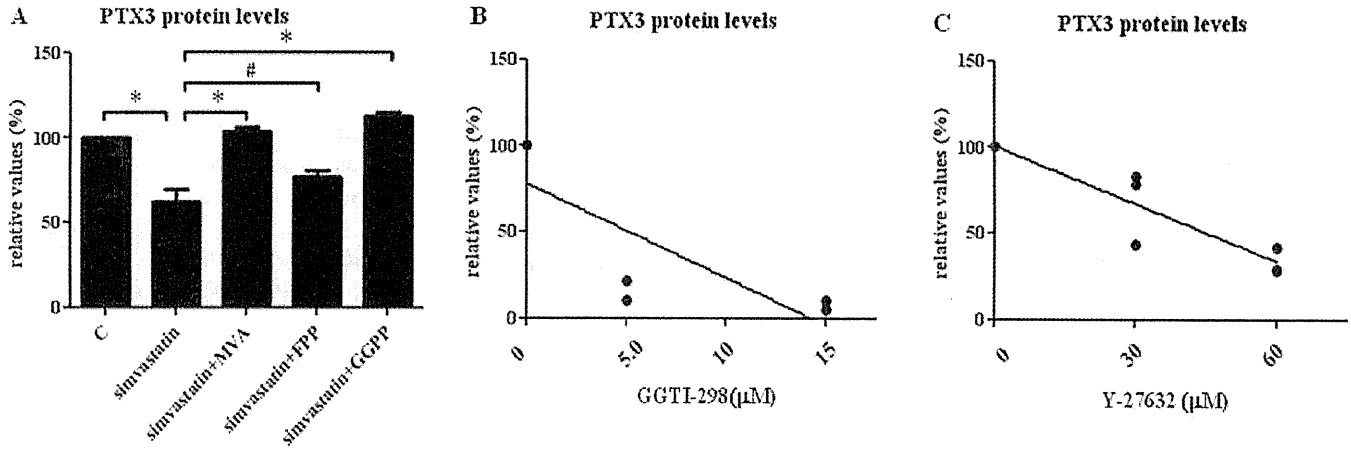

Fig. 2. Effects of MVA and isoprenoids on the simvastatin-mediated suppression of PTX3 production by FLS.
A. MVA and GGPP attenuated suppression of PTX3 production by simvastatin in RA FLS. FLS were incubated with 0.1 - 10 μM simvastatin for 24 h. PTX3 levels in culture supernatants were determined by ELISA (n=6); $^{*}p<0.05$ versus control, $^{\#}$ not significant. **B, C.** An inhibitor of geranylgeranylation, GGTI-298 (**B**), and a Rho kinase inhibitor, Y-27632 (**C**), suppressed PTX3 production in RA FLS in a dose-dependent manner. FLS were incubated with 5.0 or 15 μM GGTI-298 or with 30 or 60 μM Y-27632 for 24 h. Tendency lines are shown.

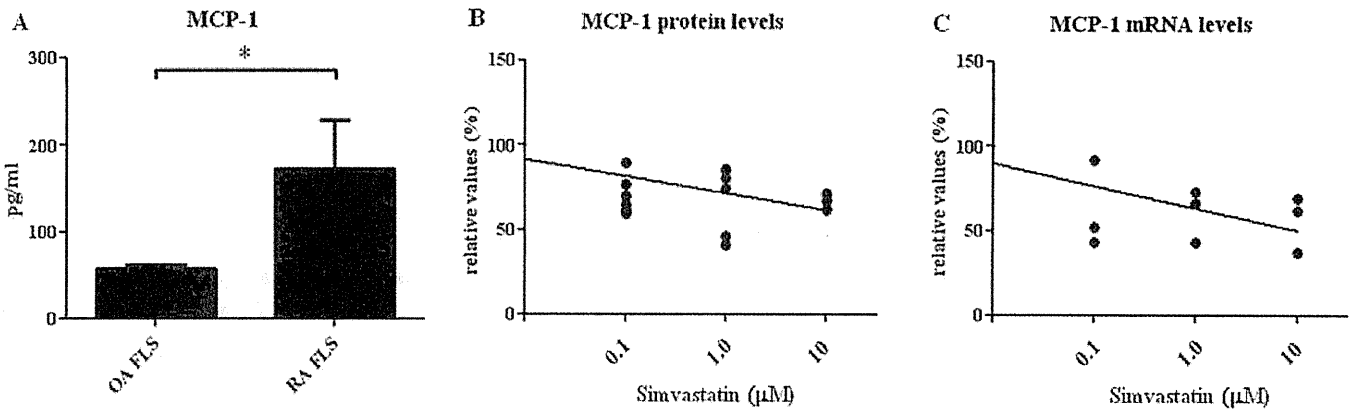

Fig. 3. RA FLS specifically produced MCP-1, which was suppressed by simvastatin.
A. FLS from patients with RA or OA were incubated without simvastatin for 24 h. MCP-1 levels in culture supernatants were determined by ELISA (n = 6); $^{*}p<0.05$ versus control. **B, C.** The expression of MCP-1 was suppressed by simvastatin in a dose-dependent manner both at the protein level (**B**, n=6) and at the mRNA level (**C**, n=3). FLS from RA patients were incubated with 0.1 - 10 μM simvastatin for 24 h. Data shown are values relative to control cells cultured in the absence of simvastatin. Tendency lines are shown.

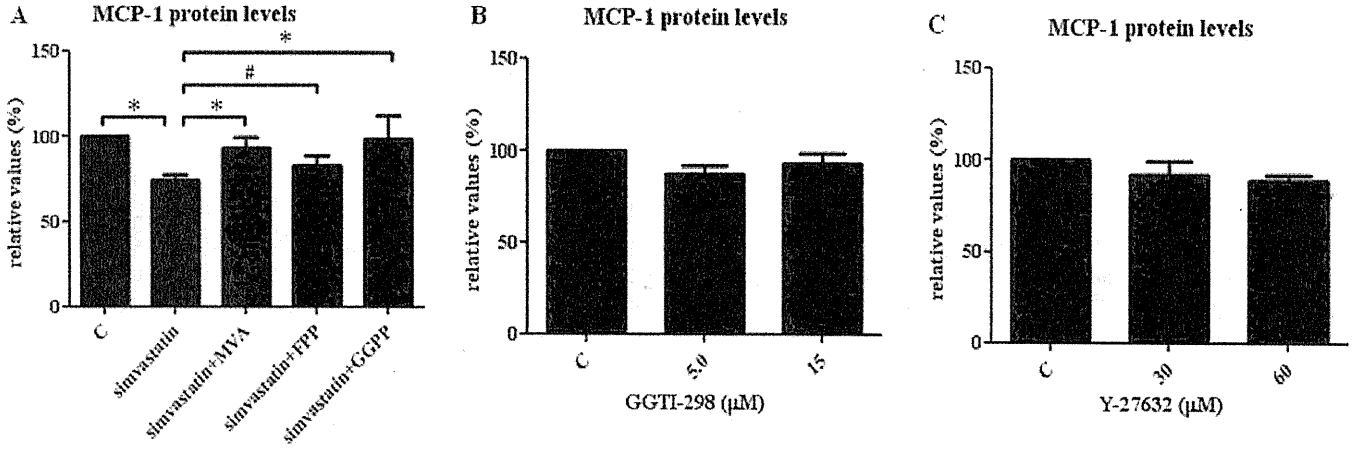

Fig. 4. Effects of MVA and isoprenoids on the simvastatin-mediated suppression of MCP-1 production by FLS.
A. MVA and GGPP attenuated suppression of MCP-1 production by simvastatin in RA FLS. FLS were incubated with 0.1–10 μM simvastatin for 24 h. MCP-1 levels in culture supernatants were determined by ELISA (n=6); $^{*}p<0.05$ versus control, $^{\#}$not significant. **B, C.** The production of MCP-1 was not affected by GGTI-298 (**B**, n=3) and Y-27632 (**C**, n=3).

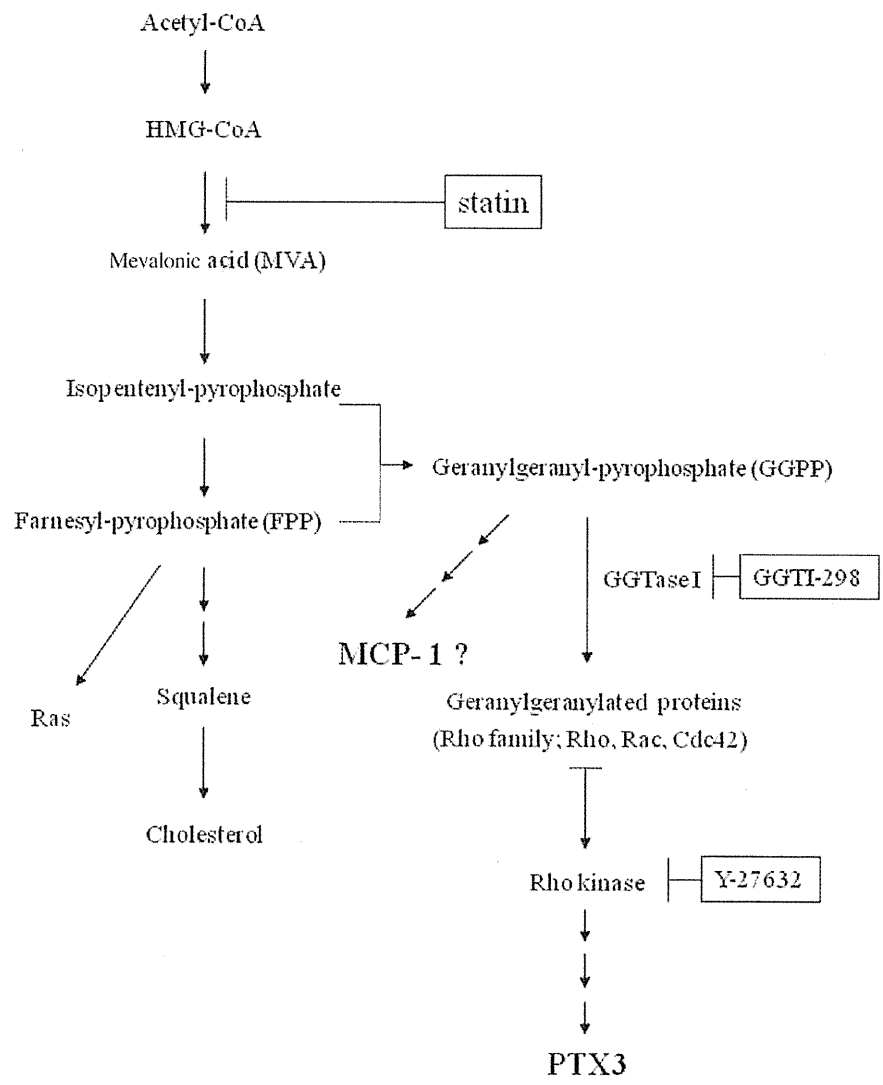

Fig. 5. Simvastatin affects FLS by two different mechanisms.
Simvastatin both reduced the secretion of PTX3 and MCP-1 in FLS. Whereas it inhibits PTX3 production in a Rho-dependent manner, it inhibits MCP-1 production in a Rho-independent manner.

on PTX3 production in the absence of simvastatin (data not shown).

Inhibitory effects of GGTI-298 and Y-27632 on PTX3 production in FLS

When FLS were incubated for 24 h with the GGTI-298, the PTX3 protein secreted into culture supernatants was reduced to 17.7±3.7% and 6.8±1.6% of control, with 5.0 μM and 15 μM GGTI-298, respectively (Fig. 2B). When FLS were incubated with Y-27632 for 24 h, PTX3 levels were reduced to 68.0±12.6% and 32.8±4.4% of control, with 30 μM and 60 μM Y-27632, respectively (Fig. 2C).

Inhibitory effects of simvastatin on MCP-1 production in RA FLS

So far, most of the molecules that we discovered to be reduced by simvastatin were regulated in a Rho-kinase dependent manner (16, 17). In our screening process, however, we also discovered a molecule, MCP-1, that was reduced by simvastatin in a Rho-kinase independent manner. The chemokine MCP-1 has been suggested to be a potential therapeutic target in RA. Its level increases in the peripheral blood, synovial fluid and synovial tissue in patients with RA, and it is known to be a potent chemoattractant for monocytes/macrophages and T cells (18).

As shown in Figure 3A, the levels of MCP-1 secreted by RA FLS after 24 h-culture in the absence of simvasta-

tin were significantly higher than those with OA.

When FLS from RA patients were incubated for 24 h with simvastatin, the MCP-1 levels in culture supernatants were reduced significantly, to 69.3±6.2%, 69.0±10.0% and 67.1±1.7%, compared with control, in the presence of 0.1 μM, 1.0 μM and 10 μM simvastatin, respectively (Fig. 3B). The expression of MCP-1 mRNA was also reduced to 62.6±15.1%, 61.0±9.3% and 56.2±9.7%, compared to controls, in the presence of 0.1 μM, 1.0 μM and 10 μM simvastatin, respectively (Fig. 3C).

MVA and GGPP restore the production of MCP-1 in FLS in the presence of simvastatin

As shown in Figure 4A, the inhibitory effect of 1.0 μM simvastatin on MCP-1 production in RA FLS attenuated if the cells were simultaneously treated by 100 μM MVA or 10 μM GGPP, but unaffected by FPP. MVA, GGPP and FPP had minimal effects on MCP-1 production in the absence of simvastatin (data not shown).

No inhibitory effects of GGTI-298 and Y-27632 on MCP-1 production in FLS

When FLS were incubated with GGTI-298 or Y-27632 for 24 h, the levels of MCP-1 were not affected by these reagents in contrast to those of PTX3 (Fig. 4B).

Discussion

In our previous reports, the production of IL-6 and IL-8 was also found to be regulated by the GGPP-dependent pathway (16). Since the expression of IL-6, IL-8 and MCP-1 in RA synovium appears to be associated with disease activity (19, 20, 21), simvastatin is thought to act via these pathways to show beneficial effects on RA patients. Furthermore, it has been demonstrated that MCP-1 is stored and released from vesicles in FLS and that high density lipoproteins (HDL) inhibit the release of MCP-1 (22). Since statins are known to increase the level of plasma HDL (23), simvastatin may inhibit both the production and release of MCP-1 from FLS.

In the present study, we have shown that simvastatin inhibited the production of PTX3 and MCP-1 on FLS from patients with RA. In addition, we have demonstrated that GGPP prevents the simvastatin-induced inhibition of PTX3 and MCP-1 production, suggesting that GGPP is critical for PTX3 and MCP-1 production in these cells. In accordance with our previous reports (16, 17), we now provide an additional evidence that simvastatin has beneficial effects on activated FLS from patients with RA.

It has been shown that the main source of PTX3 in the synovium of RA patients is pannus, in which monocytes/macrophages, FLS and endothelial cells are rich (5). It is tempting to speculate that PTX3 participates in synovial membrane injury by amplifying complement-mediated tissue damage (3). Based on these reports, our result may imply that simvastatin could improve the synovial membrane injury in RA patients.

On the other hand, among chemokines, MCP-1 is known to be a potent mediator for recruiting monocytes/macrophages and T cells (24). These cells have been shown to be directly involved in the induction and perpetuation of synovitis and subsequent joint destruction in RA (21). It has been shown that arthritis in MRL/*lpr* mice is suppressed by treating with anti-MCP-1 monoclonal antibodies before the disease-onset (25). Several lines of evidence have suggested MCP-1 plays important roles in monocyte recruitment and developing atherosclerosis (26, 27). Taken together with a poor-prognostic link between atherosclerosis and RA (28), MCP-1 may be one of the target molecules in the treatment of RA from both an anti-inflammatory and an anti-atherosclerotic aspects. Thus, simvastatin could reduce not only cardiovascular morbidity and mortality but also improve clinical measures in RA patients.

Surprisingly, treating FLS with GGTI-298 or Y-27632 significantly inhibited the production of PTX3, but had no effect on MCP-1 production. We speculated that Rho/Rho kinase may be involved in regulating the production of PTX3 but not MCP-1 in FLS (Fig. 5). In fact, it has been reported that in human endothelial cells and macrophages, statins inhibit CCR2/MCP-1 receptor expression via Rho-independent pathway (29). Therefore, in FLS it is possible that simvastatin inhibits the production of MCP-1 via Rho-independent pathway.

In conclusion, although simvastatin inhibits both PTX3 and MCP-1 production in RA FLS, the mechanisms are quite different. Simvastatin inhibits PTX3 production in a Rho-dependent manner but MCP-1 production in a Rho-independent manner. Understanding the multiple mechanisms by which simvastatin reduces these inflammatory mediators, we may be able to finely regulate the pathological conditions of patients with rheumatic diseases, such as RA.

Acknowledgements

We thank Dr Hiromi Oda and Dr Yoon Taek Kim, Department of Orthopaedic Surgery, Saitama Medical University, for providing synovial tissues, and Ms Toshiko Ishibashi and Ms Mina Sagara for technical assistance.

References

1. GARLANDA C, BOTTAZZI B, BASTONE A, MANTOVANI A: Pentraxins at the crossroads between innate immunity, inflammation, matrix deposition, and female fertility. *Annu Rev Immunol* 2005; 23: 337-66.
2. BREVIARIO F, D'ANIELLO EM, GOLAY J *et al.*: Interleukin-1-inducible genes in endothelial cells. Cloning of a new gene related to C-reactive protein and serum amyloid P component. *J Biol Chem* 1992; 267: 22190-7.
3. ORTEGA-HERNANDEZ OD, BASSI N, SHOENFELD Y, ANAYA JM: The Long Pentraxin 3 and Its Role in Autoimmunity. *Semin Arthritis Rheum* 2009; 39; 38-54.
4. PEPYS MB, HIRSCHFIELD GM: C-reactive protein: a critical update. *J Clin Invest* 2003; 111: 1805-12.
5. LUCHETTI MM, PICCININI G, MANTOVANI A *et al.*: Expression and production of the long pentraxin PTX3 in rheumatoid arthritis (RA). *Clin Exp Immunol* 2000; 119: 196-202.
6. MARON DJ, FAZIO S, LINTON MF: Current perspectives on statins. *Circulation* 2000; 101: 207-13.
7. STOSSEL TP: The discovery of statins. *Cell* 2008; 134: 903-5.
8. KWAK B, MULHAUPT F, MYIT S, MACH F: Statins as a newly recognized type of immunomodulator. *Nat Med* 2000; 6: 1399-402.
9. WEITZ-SCHMIDT G, WELZENBACH K, BRINKMANN V *et al.*: Statins selectively inhibit leukocyte function antigen-1 by binding to a novel regulatory integrin site. *Nat Med* 2001; 7: 687-92.
10. TAKEMOTO M, LIAO JK: Pleiotropic effects of 3-hydroxy-3-methylglutaryl coenzyme

a reductase inhibitors. *Arterioscler Thromb Vasc Biol* 2001; 21: 1712-9.
11. VAN AELST L, D'SOUZA-SCHOREY C: Rho GTPases and signaling networks. *Genes Dev* 1997; 11: 2295-322.
12. VOGT A, SUN J, QIAN Y, HAMILTON AD, SEBTI SM: The geranylgeranyltransferase-I inhibitor GGTI-298 arrests human tumor cells in G0/G1 and induces p21(WAF1/CIP1/SDI1) in a p53-independent manner. *J Biol Chem* 1997; 272: 27224-9.
13. MATOZAKI T, NAKANISHI H, TAKAI Y: Small G-protein networks: their crosstalk and signal cascades. *Cell Signal* 2000; 12: 515-24.
14. KANDA H, HAMASAKI K, KUBO K *et al.*: Antiinflammatory effect of simvastatin in patients with rheumatoid arthritis. *J Rheumatol* 2002; 29: 2024-6.
15. KANDA H, YOKOTA K, KOHNO C *et al.*: Effects of low-dosage simvastatin on rheumatoid arthritis through reduction of Th1/Th2 and CD4/CD8 ratios. *Mod Rheumatol* 2007; 17: 364-8.
16. YOKOTA K, MIYAZAKI T, HIRANO M, AKIYAMA Y, MIMURA T: Simvastatin inhibits production of interleukin 6 (IL-6) and IL-8 and cell proliferation induced by tumor necrosis factor-alpha in fibroblast-like synoviocytes from patients with rheumatoid arthritis. *J Rheumatol* 2006; 33: 463-71.
17. YOKOTA K, MIYOSHI F, MIYAZAKI T *et al.*: High concentration simvastatin induces apoptosis in fibroblast-like synoviocytes from patients with rheumatoid arthritis. *J Rheumatol* 2008; 35: 193-200.
18. LOETSCHER P, SEITZ M, CLARK-LEWIS I, BAGGIOLINI M, MOSER B: Monocyte chemotactic proteins MCP-1, MCP-2, and MCP-3 are major attractants for human CD4+ and CD8+ T lymphocytes. *FASEB J* 1994; 8: 1055-60.
19. BROZIK M, ROSZTÓCZY I, MERÉTEY K *et al.*: Interleukin 6 levels in synovial fluids of patients with different arthritides: correlation with local IgM rheumatoid factor and systemic acute phase protein production. *J Rheumatol* 1992; 19: 63-8.
20. KRAAN MC, PATEL DD, HARINGMAN JJ *et al.*: The development of clinical signs of rheumatoid synovial inflammation is associated with increased synthesis of the chemokine CXCL8 (interleukin-8). *Arthritis Res* 2001; 3: 65-71.
21. HARIGAI M, HARA M, YOSHIMURA T, LEONARD EJ, INOUE K, KASHIWAZAKI S: Monocyte chemoattractant protein-1 (MCP-1) in inflammatory joint diseases and its involvement in the cytokine network of rheumatoid synoviun. *Clin Immunol Immunopathol* 1993; 69: 83-91.
22. SCANU A, OLIVIERO F, GRUAZ L *et al.*: High-density lipoproteins downregulate CCL2 production in human fibroblast-like synoviocytes stimulated by urate crystals. *Arthritis Res Ther* 2010; 12: R23.
23. NICHOLLS SJ, TUZCU EM, SIPAHI I *et al.*: Statins, high-density lipoprotein cholesterol, and regression of coronary atherosclerosis. *JAMA* 2007;297:499-508.
24. ROLLINS BJ: Chemokines. *Blood* 1997; 90: 909-28.
25. GONG JH, RATKAY L G, WATERFIELD JD, CLARK-LEWIS I: An antagonist of monocyte chemoattractant protein 1 (MCP-1) inhibits arthritis in the MRL-lpr mouse model. *J Exp Med* 1997; 186: 131-7.
26. PIEMONTI L, CALORI G, LATTUADA G *et al.*: Association between plasma monocyte chemoattractant protein-1 concentration and cardiovascular disease mortality in middle-aged diabetic and nondiabetic and nondiabetic individuals. *Diabetes Care* 2009; 32: 2105-10.
27. SHANTSILA E, LIP GY: Monocytes in acute coronary syndromes. *Arterioscler Thromb Vasc Biol* 2009; 29: 1433-8.
28. BJÖRNÅDAL L, BRANDT L, KLARESKOG L, ASKLING J: Impact of parental history on patients› cardiovascular mortality in rheumatoid arthritis. *Ann Rheum Dis* 2006; 65: 741-5.
29. VEILLARD NR, BRAUNERSREUTHER V, ARNAUD C *et al.*: Simvastatin modulates chemokine and chemokine receptor expression by geranylgeranyl isoprenoid pathway in human endothelial cells and macrophages. *Atherosclerosis* 2006; 188: 51-8.

Mod Rheumatol (2010) 20:183–187
DOI 10.1007/s10165-009-0244-3

CASE REPORT

Analysis of cytokine production patterns of peripheral blood mononuclear cells from a rheumatoid arthritis patient successfully treated with rituximab

Akinori Yamamoto · Kojiro Sato · Fumihiko Miyoshi · Yasufumi Shindo · Yoshihiro Yoshida · Kazuhiro Yokota · Kyoichi Nakajima · Haruhiko Akiba · Yu Asanuma · Yuji Akiyama · Toshihide Mimura

Received: 11 March 2009 / Accepted: 1 October 2009 / Published online: 7 November 2009

Abstract We had a rheumatoid arthritis (RA) patient resistant to multiple drugs and who developed panniculitis due to etanercept treatment, then responded fairly well to rituximab. Intracellular staining of cytokines in the peripheral blood mononuclear cells before and after rituximab administration revealed that the cytokine production, representative of T-helper (Th)1-, Th2-, and Th17-type responses, decreased abruptly after the treatment. Interestingly, this timing coincided with that of the manifestation of the beneficial effect. This relationship may provide useful insight into the mechanism of action of the drug and hence about the pathogenesis of RA.

Keywords Rheumatoid arthritis · Rituximab · Th1 · Th2 · Th17

Introduction

Recently, with the advent of the so-called "biologics," the treatment of rheumatoid arthritis (RA), the most common autoimmune disease that affects and destroys joints, has undergone dramatic change. Biologics ameliorate the symptoms of RA that cannot be controlled by conventional disease-modifying antirheumatic drugs (DMARDs) and improve the patients' activities of daily living (ADL). Tumor necrosis factor (TNF) blockers spearheaded such new drugs [1, 2]. In 2008, the anti-interleukin (IL)-6 receptor antibody tocilizumab was also approved as a drug against RA in Japan [3, 4]. Furthermore, a fusion protein composed of an immunoglobulin (Ig) fused to the extracellular domain of CTLA-4 (abatacept [5]) and a monoclonal antibody against CD20, which is expressed on B cells (ocrelizumab [6]), are now undergoing clinical trials in Japan. In Europe and the USA, an anti-CD20 monoclonal antibody (rituximab [7]) and abatacept have already been approved. It is claimed that treatment with rituximab may be better for patients who exhibit an inadequate response to at least one anti-TNF agent rather than switching to an alternative anti-TNF agent [8]. Rituximab was first approved for B-cell non-Hodgkin's lymphoma, and the reason it is effective in treating RA remains unclear. Here we report a case of RA with effect attenuation of and/or intolerance to anti-TNF agents that was treated successfully with rituximab.

CD4-positive ($CD4^+$) effector T cells are typically divided into three subsets: Th1, Th2, and Th17 cells [9, 10]. Each subset plays a definitive role in the immune response. Th1 cells are mainly involved in cellular immunity, and Th2 cells are implicated in humoral immunity, including the allergic response. Th17 cells, recently identified, are considered to play important roles in certain autoimmune diseases, including RA and multiple sclerosis (MS). These subsets produce specific cytokines, and interferon gamma (IFN-γ), interleukin (IL)-4, and IL-17 are the representative cytokines of each subset. As Th17 cells have been implicated in the pathogenesis of RA, we performed a time-series assessment of the cytokine production pattern of $CD4^+$ T cells in peripheral blood mononuclear cells (PBMCs) from the patient in order to shed light on the mechanism(s) of action of rituximab in RA treatment.

A. Yamamoto · K. Sato (✉) · F. Miyoshi · Y. Shindo · Y. Yoshida · K. Yokota · K. Nakajima · H. Akiba · Y. Asanuma · Y. Akiyama · T. Mimura
Department of Rheumatology and Applied Immunology, Faculty of Medicine, Saitama Medical University Hospital, 38 Morohongo, Moroyama, Iruma-gun, Saitama 350-0495, Japan
e-mail: satok@saitama-med.ac.jp

Case report

A 64-year-old woman who had been diagnosed with RA 13 years ago and treated with various conventional DMARDs such as bucillamine, salazosulfapyridine, leflunomide (20 mg/day), and methotrexate (MTX, 2–4 mg/week) was admitted to our hospital because of severe arthritis and painful nodules under the skin. Infliximab (180 mg, along with MTX) had been introduced a year earlier but was stopped because of the attenuation of effect and the occurrence of shingles. Etanercept was then administered with good results. About 1 year later, however, numerous subcutaneous nodules with accompanying pain appeared on her limbs and trunk. Consequently, she was referred to this hospital and admitted for further examination. She had a brother and a sister who were also afflicted with RA. On examination, the patient looked ill. Her temperature was 36.4°C, pulse 80 beats per minute, and blood pressure 170/98 mmHg. Her weight was 54.6 kg and height 150 cm. Chest sounds were normal. The abdomen was flat and soft, and bowel sounds were normal. Ulnar drift deformity of the fingers was observed bilaterally. Both shoulder joints, the left elbow joint, and both ankle joints were swollen and tender. Numerous tender nodules 1–2 cm in diameter were noted under the skin of the limbs and the trunk; some of them accorded with the sites of etanercept injection. Erythrocyte sedimentation rate (ESR) was 57 mm/h, C-reactive protein (CRP) level <0.10 mg/dl, rheumatoid factor (RF) 419 IU/ml, and matrix metalloproteinase-3 (MMP-3) 534.2 ng/ml. The Disease Activity Score of 28 joints (DAS28)-CRP4 level was 6.3 and DAS28-ESR4 7.46. CRP level was not high, probably because of etanercept treatment until just before the admission. Functional class was estimated to be class III and radiographic stage was assessed as stage II. Infectious conditions including cutaneous tuberculosis were unlikely in light of negative tuberculin test and other cultivation tests. Skin biopsy was performed and revealed diffuse changes in subcutaneous adipose tissue with the infiltration of inflammatory cells, mostly lipophages, indicating a chronic lobular panniculitis. No vasculitis was present. A side effect of etanercept was suspected, and the skin lesions subsided gradually after cessation of the agent.

The arthralgia, however, became poorly controlled. Despite the increased dose of glucocorticoid (betamethasone 1.0 mg/day to 2.0 mg/day), inflammatory maker levels were gradually elevated and settled at as high as 10 mg/dl for CRP and 100 mm/h for ESR. DAS28 also increased and reached 6.21 (CRP4) and 7.27 (ESR4) 4 month after admission. She became almost bedridden because of arthralgia. By that time, tacrolimus, MTX, and salazosulfapyridine had been tried one after another in turn but had to be stopped because of side effects (deterioration in renal function, abdominal and dorsal eruption, and fever and eruption, respectively). To relieve the pain, glucocorticoid injection was performed almost every 2 weeks (8 mg of dexamethasone sodium phosphate intra-articularly, 4 mg of dexamethasone palmitate intravenously, or 40 mg triamcinolone acetonide intra-articularly), without lasting effect (Fig. 1a).

Finally, we decided to use rituximab because there was no other biologic available at that time (in 2007). After obtaining permission of the medical ethics board at this hospital, 500 mg of rituximab was administered intravenously twice in 2 weeks. Ibuprofen (200 mg) and DL-chlorpheniramine maleate (2 mg) were administered orally and hydrocortisone sodium succinate (100 mg) intravenously as prophylactic medication. Except for flushing of the face, no apparent injection reaction was observed. Before the second injection, the number of B cells ($CD19^+$ cells) in the peripheral blood dropped from 150/μl to <10/μl. This decrease was irrespective of the expression of an activation marker CD38 (Fig. 1b). For approximately 1 month after the treatment, no improvement was detected either subjectively or objectively. After that, however, the level of CRP decreased to <0.1 mg/dl fairly abruptly, and levels of ESR and RF were reduced also, although more gradually (Fig. 1a).

The numbers of $CD4^+$ and $CD8^+$ T cells in the peripheral blood were not significantly affected by rituximab. To estimate the pattern of Th response before and after rituximab treatment, we performed flow cytometric analysis of intracellular cytokines, namely, IFN-γ, IL-4, and IL-17, in $CD4^+$ cells (Fig. 2). PBMCs were separated by a centrifugation method using Ficoll–Conray solution (Lymphosepal, Immuno-Biological Laboratories, Japan). PBMCs were cultured in the Roswell Park Memorial Institute (RPMI) 1640 medium supplemented with 10% fetal bovine serum (FBS) in the presence of phorbol myristate acetate (PMA, 40 ng/ml) and ionomycin (1 μg/ml) for 5 h. During the last 1 h, monensin [Golgistop, Becton, Dickinson (BD) Bioscience, USA] was added to the culture. After that, cells were stained with anti-CD4- phycoerythrin/cytochrome 5 (PE/Cy5), and intracellularly stained with anti-IFN-γ fluorescein isothiocyanate (FITC) and either anti-IL-4-PE or anti-IL-17-PE (all reagents were from BD Bioscience). The cells were then analyzed using a FACSCan (BD Bioscience). Interestingly, the rate of cytokine-positive cells dropped suddenly 1 month after the treatment. The decrease in the number of IL-4-positive cells was the greatest: >90%. IL-17- or IFN-γ-positive cells were decreased by approximately 80% and 40%, respectively. The levels of IL-4 and IL-17 detected in the supernatant of the cells stimulated in vitro (without the addition of monensin) also dropped drastically, although that of IFN-γ did not decrease significantly (data not

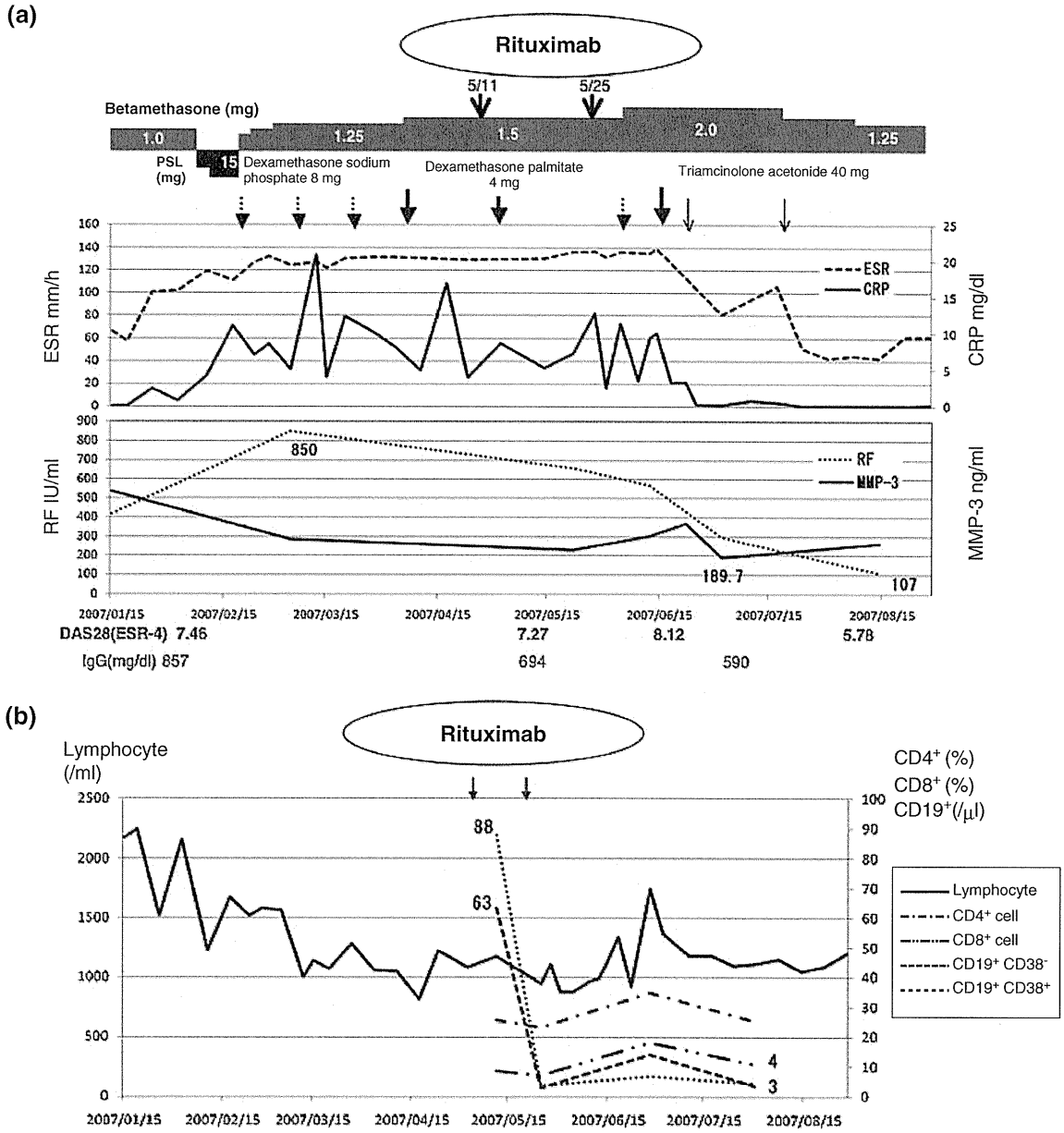

Fig. 1 Clinical course of the patient (**a**) and time course of the numbers of total lymphocytes, $CD19^+CD38^+$ B cell, and $CD19^+$ $CD38^-$ B cell (/μl), and the ratio of $CD4^+$ and $CD8^+$ cells (%) in the peripheral blood (**b**). Although rituximab dramatically reduced the number of circulating B cells, it did not significantly affect the number of $CD4^+$ and $CD8^+$ cells. *PSL* prednisolone

shown). Thus, although the decrease in the rate (and fluorescence intensity) of IFN-γ-positive cells may have little significance, those of IL-4- and IL-17-positive cells are likely to be functionally significant. Two months after the treatment, the rates of cytokine-positive cells returned to nearly the former values. Four months after the treatment, the number of B cells remained low, and the levels of CRP and ESR were <0.10 mg/dl and 22 mm/h, respectively, regardless of the fact that we tapered the dose of betamethasone to 1.5 mg. DAS28 at the time of discharge was 4.69 (CRP4) and 5.97 (ESR4); the patient's subjective symptoms did not improve much, although her objective symptoms, including joint swelling and warmth, had subsided greatly. She was followed at the previous clinic and about 1 year after the second injection of rituximab, she began to be treated with adalimumab (40 mg/2 weeks). It was tolerated well and proved effective in maintaining her ADL thereafter.

Discussion

The effects of rituximab on this patient have two outstanding characteristics. First, the effects were rather slow

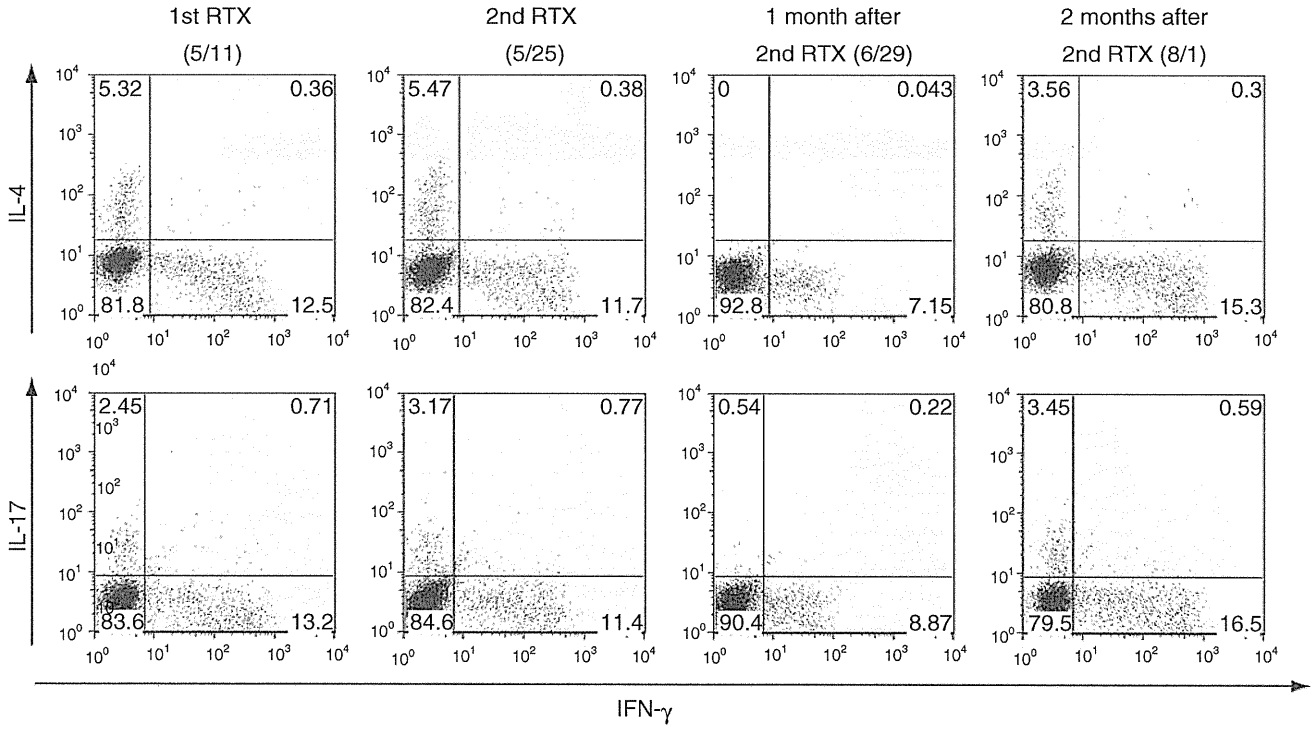

Fig. 2 Flow cytometric analysis of the intracellular cytokines in $CD4^+$ peripheral blood mononuclear cells (PBMCs) derived from the patient. Compared with data on the first day (11 May) of rituximab (RTX) treatment, the frequency of cytokine-positive cells was decreased significantly 1 month after the second RTX treatment (29 June)

to appear; it took almost 1 month for inflammatory markers to start dropping. This result is consistent with the report by Edwards et al. [7] and stands in striking contrast to the rapid onset of TNF blockers such as infliximab [11]. Cambridge et al. [12] reported that with rituximab treatment, Ig levels do not drop significantly, whereas those of anticyclic citrullinated peptide antibody (anti-CCP Ab) and RF dropped significantly but gradually. Autoantibodies increased just after the recovery of B cell number, and then the symptoms of RA relapsed. As CRP level decrease preceded that of the autoantibodies, however, the decrease of autoantibody levels might be interpreted not as a cause of but rather as a result of RA amelioration. Consistent with this, the transfer of large amounts of serum from patients with active RA, which contained RF, failed to induce any disease in the recipients, suggesting that antibodies including RF do not represent major effector mechanisms in RA [13]. It was also reported that rituximab was effective not only in RF-positive patients but also in RF-negative patients [14]. These results suggest that it is not the antibodies produced by B cells, but rather, the B cells themselves that are implicated in the pathogenesis of RA. For example, B cells may function as antigen-presenting cells. Alternatively, they may be required for the formation of lymph-node-like structures observed in the synovium of RA joints [15].

From this perspective, it is interesting that cytokine production from Th cells in the peripheral blood of our patient dropped, transiently, about 1 month after rituximab treatment, just when the desirable effects of the agent became apparent (Fig. 2). As far as we know, this is the first report on the relationship between treatment of RA with rituximab and the Th-cytokine production profile. Although the number of Th cells in the peripheral blood did not change significantly during this period (Fig. 1b), the B cell–T cell axis is likely to play an important role in maintaining the pathological conditions of RA. Recently, Th17 cells have been implicated in the pathogenesis of certain autoimmune diseases, including RA and MS; however, the decrease in cytokine-producing cells was not IL-17 specific. Rather, the number of IL-4-producing cells dropped the most. Thus, judging from the PBMC data alone, the importance of Th17 cells in the pathogenesis of RA is obscure. Of course, it should be noted that these responses were observed in PBMCs, not at the specific site(s) where inflammation occurred. What is precisely happening in the affected joints remains an interesting issue that is open to investigation. As an anti-CD20 antibody called ocrelizumab, similar to rituximab, is now under evaluation in a clinical trial worldwide, including Japan, we expect to be able to analyze further the cytokine

production patterns of patients treated with ocrelizumab in the near future.

Conflict of interest statement None.

References

1. Elliott MJ, Maini RN, Feldmann M, Kalden JR, Antoni C, Smolen JS, et al. Randomised double-blind comparison of chimeric monoclonal antibody to tumour necrosis factor alpha (cA2) versus placebo in rheumatoid arthritis. Lancet. 1994;344:1105–10.
2. Moreland LW, Baumgartner SW, Schiff MH, Tindall EA, Fleischmann RM, Weaver AL, et al. Treatment of rheumatoid arthritis with a recombinant human tumor necrosis factor receptor (p75)-Fc fusion protein. N Engl J Med. 1997;337:141–7.
3. Nishimoto N, Yoshizaki K, Miyasaka N, Yamamoto K, Kawai S, Takeuchi T, et al. Treatment of rheumatoid arthritis with humanized anti-interleukin-6 receptor antibody: a multicenter, double-blind, placebo-controlled trial. Arthritis Rheum. 2004;50:1761–9.
4. Smolen JS, Beaulieu A, Rubbert-Roth A, Ramos-Remus C, Rovensky J, Alecock E, et al. Effect of interleukin-6 receptor inhibition with tocilizumab in patients with rheumatoid arthritis (OPTION study): a double-blind, placebo-controlled, randomised trial. Lancet. 2008;371:987–97.
5. Kremer JM, Genant HK, Moreland LW, Russell AS, Emery P, Abud-Mendoza C, et al. Effects of abatacept in patients with methotrexate-resistant active rheumatoid arthritis: a randomized trial. Ann Intern Med. 2006;144:865–76.
6. Genovese MC, Kaine JL, Lowenstein MB, Giudice JD, Baldassare A, Schechtman J, et al. Ocrelizumab, a humanized anti-CD20 monoclonal antibody, in the treatment of patients with rheumatoid arthritis: a phase I/II randomized, blinded, placebo-controlled, dose-ranging study. Arthritis Rheum. 2008;58:2652–61.
7. Edwards JC, Szczepanski L, Szechinski J, Filipowicz-Sosnowska A, Emery P, Close DR, et al. Efficacy of B-cell-targeted therapy with rituximab in patients with rheumatoid arthritis. N Engl J Med. 2004;350:2572–81.
8. Finckh A, Ciurea A, Brulhart L, Kyburz D, Moller B, Dehler S, et al. B cell depletion may be more effective than switching to an alternative anti-tumor necrosis factor agent in rheumatoid arthritis patients with inadequate response to anti-tumor necrosis factor agents. Arthritis Rheum. 2007;56:1417–23.
9. Sato K. Th17 cells and rheumatoid arthritis—from the standpoint of osteoclast differentiation. Allergol Int. 2008;57:109–14.
10. Weaver CT, Hatton RD, Mangan PR, Harrington LE. IL-17 family cytokines and the expanding diversity of effector T cell lineages. Annu Rev Immunol. 2007;25:821–52.
11. Lipsky PE, van der Heijde DM, St Clair EW, Furst DE, Breedveld FC, Kalden JR, et al. Infliximab and methotrexate in the treatment of rheumatoid arthritis. Anti-Tumor Necrosis Factor Trial in Rheumatoid Arthritis with Concomitant Therapy Study Group. N Engl J Med. 2000;343:1594–602.
12. Cambridge G, Leandro MJ, Edwards JC, Ehrenstein MR, Salden M, Bodman-Smith M, et al. Serologic changes following B lymphocyte depletion therapy for rheumatoid arthritis. Arthritis Rheum. 2003;48:2146–54.
13. Harris J, Vaughan JH. Transfusion studies in rheumatoid arthritis. Arthritis Rheum. 1961;4:47–55.
14. Cohen SB, Emery P, Greenwald MW, Dougados M, Furie RA, Genovese MC, et al. Rituximab for rheumatoid arthritis refractory to anti-tumor necrosis factor therapy: results of a multicenter, randomized, double-blind, placebo-controlled, phase III trial evaluating primary efficacy and safety at twenty-four weeks. Arthritis Rheum. 2006;54:2793–806.
15. Manzo A, Pitzalis C. Lymphoid tissue reactions in rheumatoid arthritis. Autoimmun Rev. 2007;7:30–4.

Cancer Chemother Pharmacol (2011) 67:237–241
DOI 10.1007/s00280-010-1445-3

SHORT COMMUNICATION

The small-molecule tyrosine kinase inhibitor nilotinib is a potent noncompetitive inhibitor of the SN-38 glucuronidation by human UGT1A1

Ken-ichi Fujita · Minako Sugiyama · Yuko Akiyama · Yuichi Ando · Yasutsuna Sasaki

Received: 22 June 2010 / Accepted: 20 August 2010 / Published online: 2 September 2010

Abstract
Purpose Inhibition of the UDP-glucuronosyltransferase (UGT) 1A1 by nilotinib was examined in vitro with SN-38 as a substrate, to estimate the possibility of drug–drug interaction of nilotinib with other medicines predominantly detoxified by UGT1A1.
Methods Inhibition of UGT1A1-catalyzed SN-38 glucuronidation by nilotinib was examined with human liver microsomes (HLM) and recombinant human UGT1A1 as enzyme sources. Inhibition constants (K_i) were estimated with kinetic analysis.
Results Nilotinib potently inhibited the SN-38 glucuronidation by human liver microsomal UGT1A1 and recombinant UGT1A1 in a noncompetitive manner, with K_i values of 0.286 ± 0.0094 and 0.079 ± 0.0029 μM, respectively. If a drug that serves as a substrate of UGT1A1 is administered with nilotinib, the area under the plasma concentration–time curve of a drug estimated by using these K_i values would be two times or higher than that without nilotinib, suggesting drug–drug interactions involving UGT1A1. These in vitro data and the prediction of drug–drug interaction are helpful for the clinical management of the nilotinib use.
Conclusion We found that nilotinib is a potent noncompetitive inhibitor of human UGT1A1 activity.

Keywords Nilotinib · UGT1A1 · Inhibition · Drug–drug interaction · SN-38

K. Fujita (✉) · M. Sugiyama · Y. Akiyama · Y. Sasaki
Department of Medical Oncology, International Medical Center, Comprehensive Cancer Center, Saitama Medical University, 1397-1 Yamane, Hidaka, Saitama 350-1298, Japan
e-mail: fujitak@saitama-med.ac.jp

K. Fujita · M. Sugiyama · Y. Akiyama · Y. Sasaki
Project Research Laboratory, Research Center for Genomic Medicine, Saitama Medical University, 1397-1 Yamane, Hidaka, Saitama 350-1241, Japan

Y. Ando
Department of Clinical Oncology and Chemotherapy, Nagoya University Hospital, 65 Tsurumai-Cho, Showa-Ku, Nagoya 466-8560, Japan

Introduction

Drug–drug interactions have received increasing attention over the past few decades. A recent survey indicated that more than 30% of the US population over 57 years of age takes at least five prescription drugs at any given time. Drug–drug interactions contributed to the toxicity of some drugs that were withdrawn from the US market. Many of these interactions involved inhibition of drug-metabolizing enzymes and transporters, resulting in increased systemic exposure and subsequent adverse drug reactions [1]. Therefore, the evaluation of drug–drug interaction potential is an essential part of risk assessment for the better clinical management of the use of medicines.

Nilotinib is a small-molecule multiprotein tyrosine kinase inhibitor, targeting the Bcr-Abl fusion protein, c-Kit, platelet-derived growth factor receptor (PDGFR) α, and PDGFR β [2, 3], which is approved for the treatment of Bcr-Abl positive CML in adult patients resistant to or intolerant of prior therapy that included imatinib [4]. One study has suggested that nilotinib might inhibit UDP-glucuronosyltransferase (UGT) 1A1 to cause hyperbilirubinemia [5]. If nilotinib is a potent inhibitor of UGT1A1, physicians should pay attention to the drug–drug interactions between nilotinib and other medicines that served as

substrate of UGT1A1. The inhibition of estradiol glucuronidation by nilotinib was previously studied in vitro (European Medicines Agency; http://www.ema.europa.eu/ema/index.jsp?curl=pages/home/Home_Page.jsp&murl=&mid=). However, there has been no report demonstrating the details of the in vitro study. Furthermore, there is no quantitative estimation of the nilotinib-induced drug–drug interactions with the K_i value obtained in the in vitro study.

Therefore, in the present study, we assessed the inhibition of UGT1A1 activity by nilotinib in vitro using SN-38 as a substrate. Human liver microsomes (HLM) and recombinant human UGT1A1 were used as the source of UGT1A1. We further quantitatively estimated the possibility of nilotinib-induced drug–drug interaction.

Methods

Chemicals

Nilotinib, SN-38, and SN-38 glucuronide (SN-38G) were purchased from Toronto Research Chemicals (North York, Canada). Camptothecin was from Wako (Tokyo, Japan). UGT reaction mix solution A (25 mM UDP-glucuronic acid [UDPGA] cofactor) and UGT reaction mix solution B (5×-UGT buffer mix with alamethicin, 250 mM Tris–HCl, 40 mM $MgCl_2$, and 0.125 mg/mL alamethicin in water) were from BD Biosciences (Woburn, MA). All chemicals and solvents were of the highest grade commercially available.

Human liver microsomes and recombinant human UGT1A1

Pooled HLM were purchased from BD Biosciences (Woburn, MA). The pooled HLM were derived from 24 donors (92% Caucasian, 4% Hispanic, and 4% African-American; 17 men and 7 women) with a median age of 45 years (range, 16–77). Microsomes were diluted in 250 mM sucrose. Microsomal protein content was 20 mg/mL. Estradiol 3-glucuronidation by the liver microsomes measured by BD Biosciences (Woburn, MA) was 720 pmol/min/mg prot. Recombinant human UGT1A1 supersomes expressed in baculovirus-infected insect cells were obtained from BD Biosciences (Woburn, MA). Microsomal protein content was 5.0 mg/mL.

Inhibition assay of SN-38 glucuronidation

Based on the linear relation between the human liver microsomal protein concentration and the reaction time versus the amount of metabolite formation, the protein content and the reaction time were set at 0.5 mg/mL and 5 min, respectively. In the case using the recombinant human UGT1A1 as an enzyme source, the protein content and the reaction time were at 0.2 mg/mL and 30 min, respectively.

The effects of nilotinib on SN-38 glucuronidation by HLM or the recombinant human UGT1A1 were assessed as follows: After preincubation of the incubation mixture with nilotinib or solvent dimethyl sulfoxide (DMSO) at 37°C for 5 min, the substrate SN-38 dissolved in 1% DMSO was added. Nilotinib was dissolved in DMSO. The final concentration of the solvent in the reaction mixture was 1.1%. SN-38 glucuronidation by HLM or recombinant human UGT1A1 was assayed using BD Biosciences (Woburn, MA) products, as described in the UGT reaction mix solution A or B protocol. The typical incubation mixture consisted of 50 mM Tris–HCl buffer (pH 7.5), 8 mM $MgCl_2$, 25 μg/mL alamethicin, 2 mM UDPGA, and microsomal fractions of human liver or the recombinant human UGT1A1 in a final volume of 0.2 mL. The reaction was terminated by adding a twofold volume of acetonitrile. Each assay was performed three times in duplicate.

HPLC analysis for SN-38 glucuronide

SN-38G was analyzed by HPLC using a computerized HPLC system (Hitachi model 7000 series, Hitachi, Tokyo, Japan) equipped with a TSK-gel ODS-120T analytical column (4.6 × 250 mm; 4 μm; TOSOH, Tokyo, Japan), as described elsewhere [6]. The mobile phase consisted of 75 mM ammonium acetate (pH 4.75) for solvent A and acetonitrile for solvent B. The metabolite was separated using a linear gradient of 85–65% solvent A, a time of 0–25 min, and a flow rate of 1.0 mL/min. The metabolite was quantified by comparing the HPLC peak area to that of the internal standard camptothecin. The lower limit of quantification was 0.49 nM for SN-38G. The intra- and inter-assay coefficients of variation at 4.0 nM were less than 4.2 and 12.2%, respectively.

Estimation of enzyme and inhibition kinetics

When the HLM were used to estimate the enzyme kinetics (K_m and V_{max}) of SN-38 glucuronidation by UGT1A1 or to determine the K_i of nilotinib for UGT1A1-catalyzed SN-38 glucuronidation, SN-38 concentrations ranged from 2.5 to 40 μM in the absence or presence of an inhibitor (0.125–1 μM). In the case of using the recombinant human UGT1A1, SN-38 concentrations ranged from 1.25 to 40 μM in the absence or presence of an inhibitor (0.025–0.2 μM).

Michaelis–Menten equation was fitted to data points to estimate the K_m and V_{max} values by nonlinear least-squares regression analysis, performed with GraphPad Prism version 5 software (GraphPad Software). The K_i values were also calculated by nonlinear regression analysis with